Spin-orbit torque in magnetic heterostructures: spin filtering detection of antiferromagnetic resonance and ultrasensitive Sagnac Kerr interferometry

Yunqiu Kelly Luo

Gabilan Assistant Professor
Department of Physics and Astronomy
Department of Chemistry
Mork Family Department of Chemical Engineering and Materials Science
University of Southern California

kelly.y.luo@usc.edu
Ultrafast Quantum Opto-Spintronics Group at USC:
https://sites.usc.edu/kellyluolab/

The zoo of 2D van der Waals materials

2004: Graphene

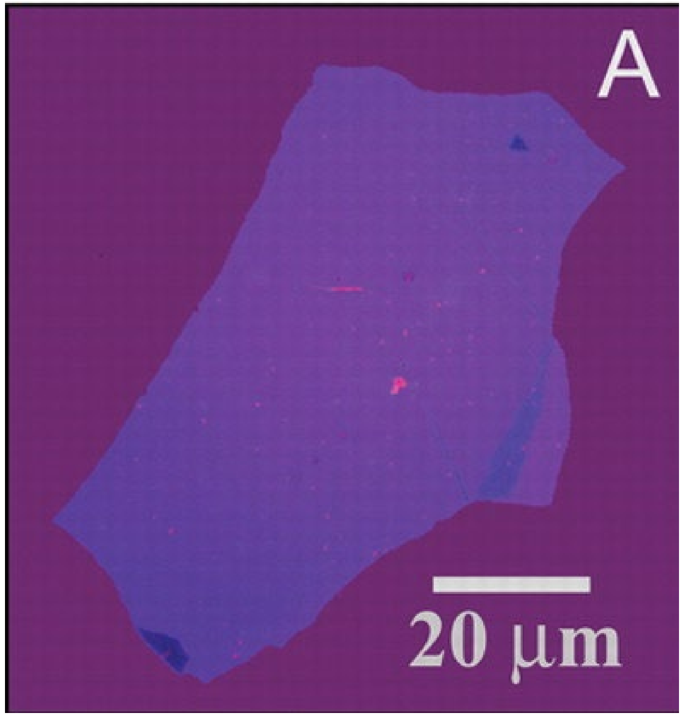

Novoselov, Kostya S., et al. "Electric field effect in atomically thin carbon films." *science* 306.5696 (2004): 666-669.

2010: TMDs (Transition Metal Dichalcogenides)

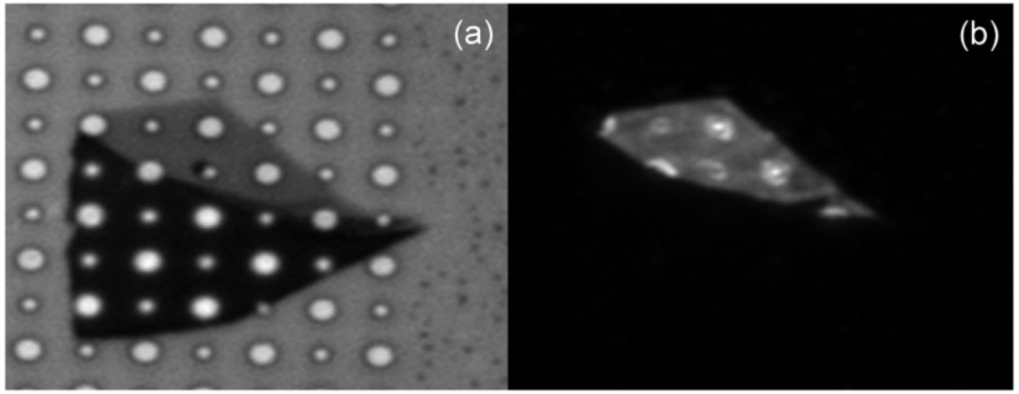

Splendiani, Andrea, et al. "Emerging photoluminescence in monolayer MoS2." *Nano letters* 10.4 (2010): 1271-1275.
Mak, Kin Fai, et al. "Atomically thin MoS2 : a new direct-gap semiconductor." *Physical review letters* 105.13 (2010): 136805.

2017: Magnets

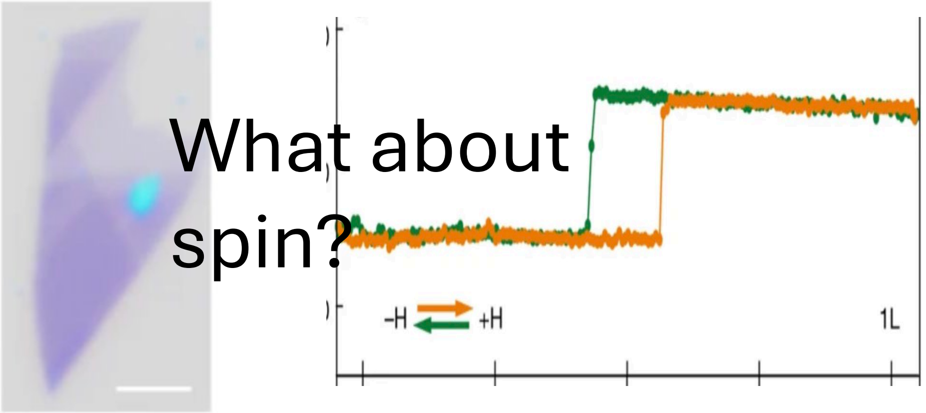

What about spin?

Huang, Bevin, et al. "Layer-dependent ferromagnetism in a van der Waals crystal down to the monolayer limit." *Nature* 546.7657 (2017): 270-273.

2D magnetic heterostructures for exploring new interfacial phenomena and technologies

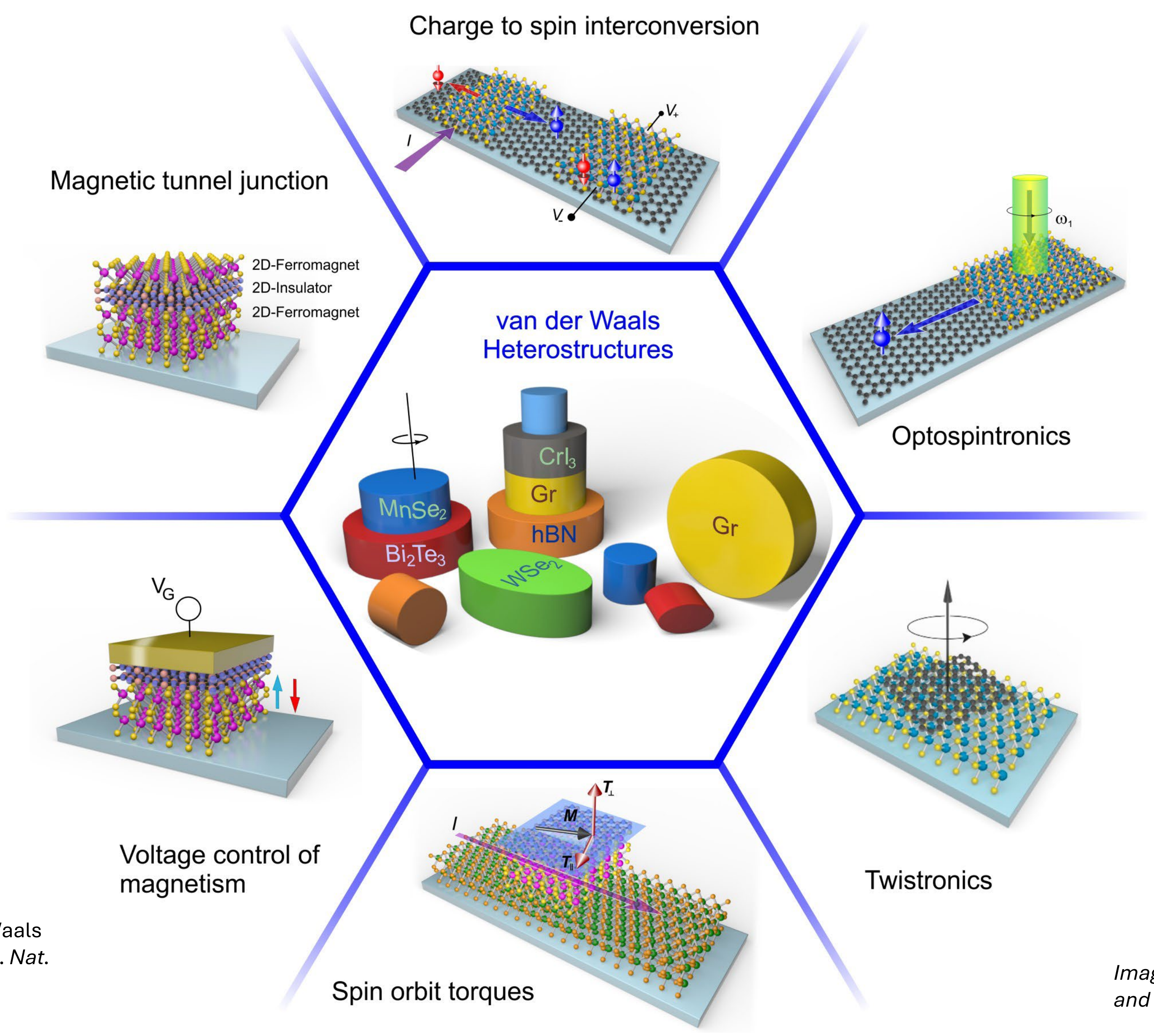

Sierra, J.F., Fabian, J., Kawakami, R.K. *et al.* Van der Waals heterostructures for spintronics and opto-spintronics. *Nat. Nanotechnol.* **16**, 856–868 (2021). https://doi.org/10.1038/s41565-021-00936-x

Image from Catalan Institute of Nanoscience and Nanotechnology

Ultrafast Quantum Opto-Spintronics Lab at the University of Southern California

Two Helium-free scanning optical microscope with superconducting vector magnets:
1) Attodry 2100: 9-1-1 T
2) Cryomagnetics Vari-6-1-1 T

Ultrafast lasers (visible to mid-IR):
1) Ti:sapphire OPO
2) Crogenic Sagnac Kerr scanning interferometry

- **Glovebox** to be connected with **UHV suitcase** for air-free interface with beamline work.

- **HQ graphene automatic transfer stage.**

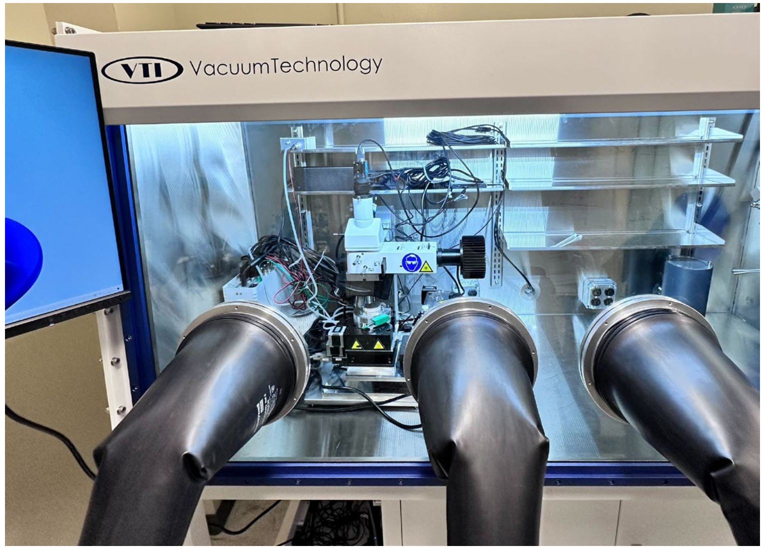

We are recruiting! https://sites.usc.edu/kellyluolab/

USC CORE NANOFABRICATION FACILITIES
Viterbi School of Engineering

National and International User Facilities:

Visit us at: Ultrafast Quantum Opto-Spintronics Group at USC
https://sites.usc.edu/kellyluolab/

NSF National Extreme Ultrafast Science Facility (NeXUS) at Ohio State:

What's the dynamic processes of electron and spin correlations?

- **Time-resolved angle-resolved photoelectron spectroscopy (tr-ARPES):**

  1 kW laser, attosecond and femtosecond pulse, up to 100 eV, spectral resolution < 30 meV

Bessy II Synchrotron MAgnetic X-raY Microscope with UHV Spectroscopy (MAXYMUS):

What's the information processing speed in the atomically thin magnets?

- **Time-resolved scanning transmission X-ray microscope (tr-STXM):**
  captures element-specific magnetization dynamics with femtosecond time resolution.

Molecular Foundry - Lawrence Berkeley National Lab:

What's the nanoscale surface spin texture?

- **Spin-Polarized Low-Energy Electron Microscope (qSPLEEM):**
  spin-resolved magnetic imaging of the unoccupied state down to 20 nm.

Manipulating magnetic materials using electron spins

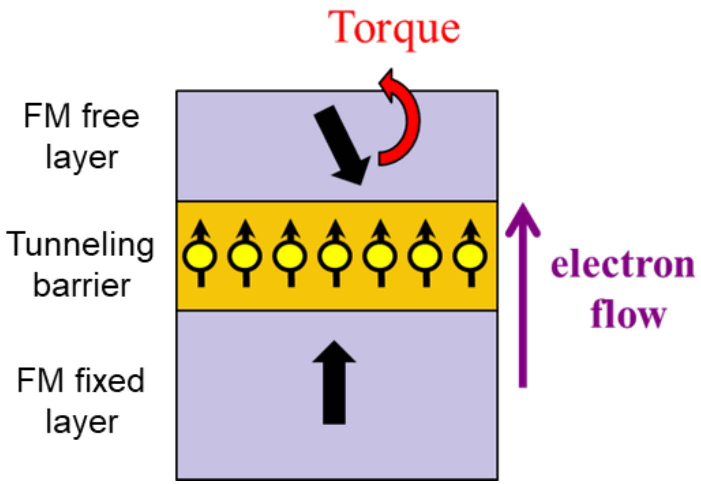

Everspin Technologies

Spin Transfer Torque

- Existing MRAM technology: Major silicon foundries offer as a standard option for embedded applications in 2018-19.
- Fundamental maximum efficiency is 1 unit of $\hbar/2$ per unit of charge in current

Spin-orbit Torque:

- Use a non-magnetic material to generate spin current
- Efficiency no longer limited to $\hbar/2e$

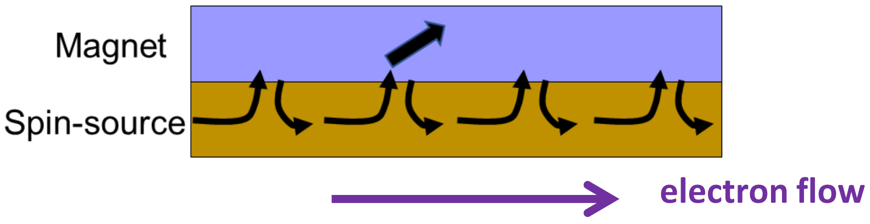

- “Spin-source” is typically a material with large spin-orbit coupling

Spin-momentum locking in topological surface states

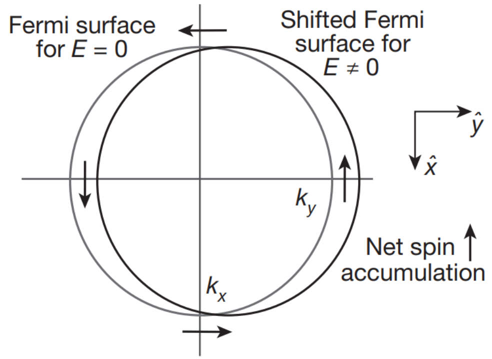

Bulk spin Hall effect

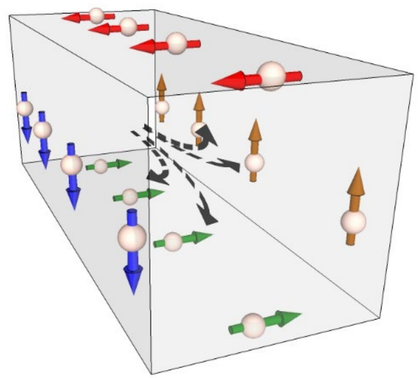

Mellnik, Ralph *et al.* Nature (2014)
Fan, Tserkovnyak, Wang *et al.* Nature Mater. (2014)

Outline

Electrical detection of antiferromagnetic resonance with electrically-tunable damping

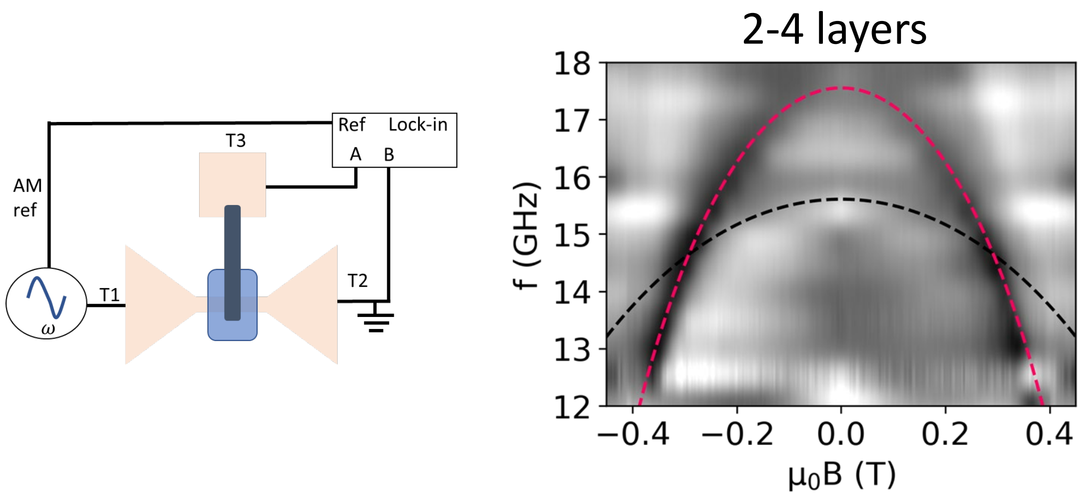

Nano Letters, *22*(16), 6716-6723 (2022);
Advanced Materials. 2305739 (2024)
arXiv: 2407.09462. Science (2025).
DOI: 10.1126/science.adq8590

High-sensitivity optical SOT metrology: Sagnac Kerr interferometry

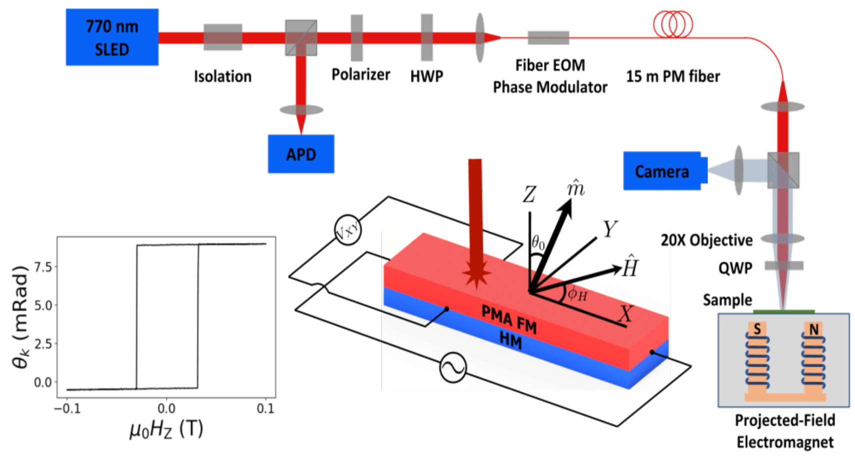

Science Advances 9(36), eadi9039 (2023);
First version: arXiv: 2109.13759 (2021)

Outline

Electrical detection of antiferromagnetic resonance with electrically-tunable damping

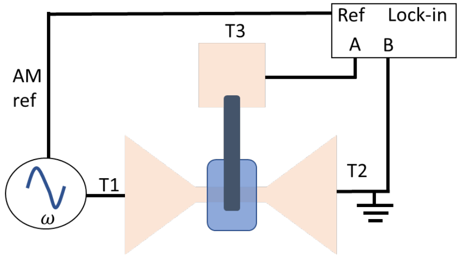

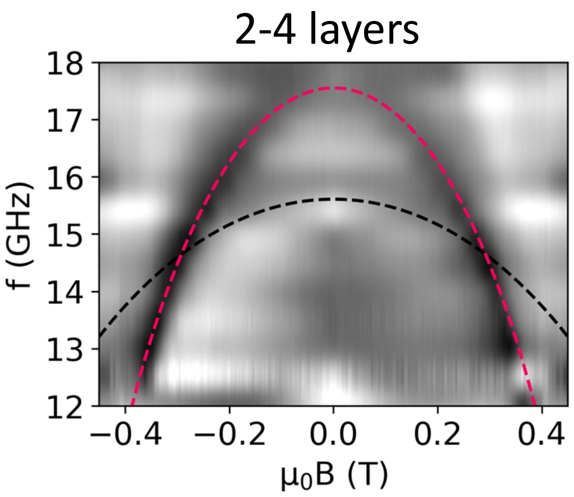

Nano Letters, ***22***(16), 6716-6723 (2022);
Advanced Materials. 2305739 (2024)
arXiv: 2407.09462. Science (2025).
DOI: 10.1126/science.adq8590

High-sensitivity optical SOT metrology: Sagnac Kerr interferometry

Science Advances 9(36), eadi9039 (2023);
First version: arXiv: 2109.13759 (2021)

Antiferromagnetic Spintronics: The Next Frontier

Antiferromagnets vs ferromagnets:

1) Zero net magnetization: Stable to perturbation from external field.
2) Exchange coupling between sublattices:
   - Richer variety of resonance modes and mode-mode coupling.
   - Faster dynamics over a wide range (GHz to THz).

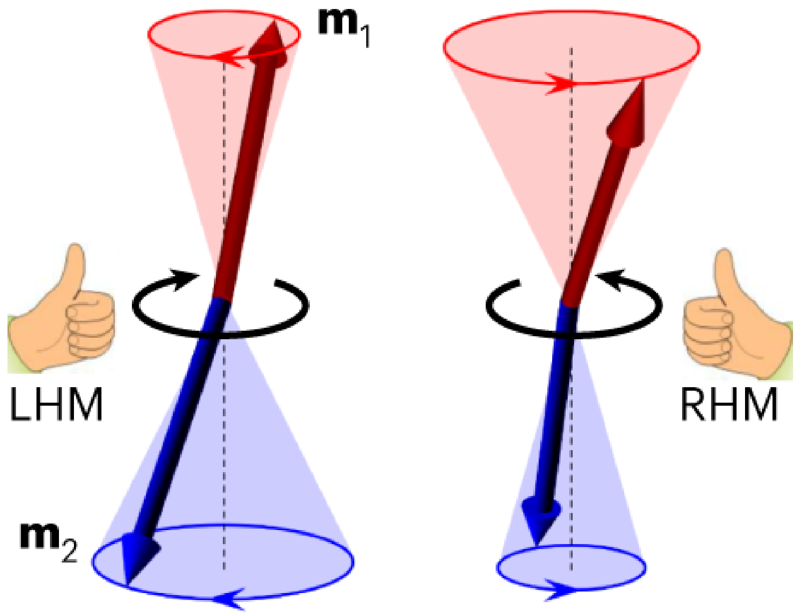

Han, J., Cheng, R., Liu, L., Ohno, H., & Fukami, S. (2023). Coherent antiferromagnetic spintronics. *Nature Materials*, *22*(6), 684-695.

Baltz, V., Manchon, A., Tsoi, M., Moriyama, T., Ono, T., & Tserkovnyak, Y. (2018). Antiferromagnetic spintronics. *Reviews of Modern Physics*, *90*(1), 015005.

Spin-Orbit Torque Control of Antiferromagnetic Resonance (AFMR)

1

Electrical detection of AFMR using spin-filter tunneling resistance

2

Spin-Orbit torque Modulation of Antiferromagnetic Resonance

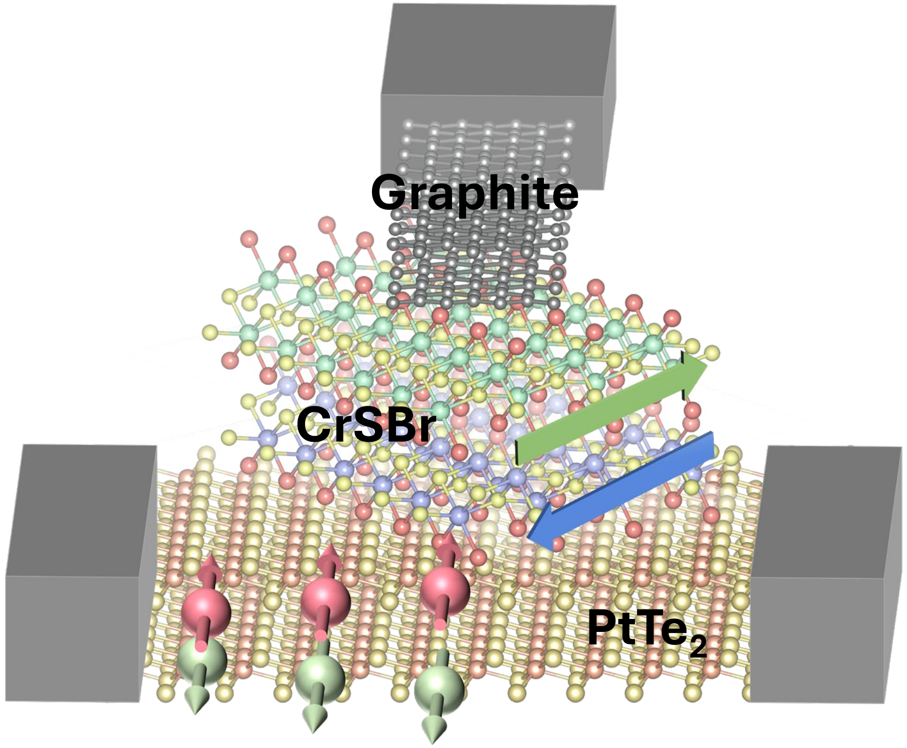

Cham, T. M. J., Huang, X., Chica, D. G., Watanabe, K., Taniguchi, T., Roy, X., Luo, Y. K., & Ralph, D. C. "Spin-filter tunneling detection of antiferromagnetic resonance with electrically-tunable damping" *arXiv:2407.09462*. Science (2025). DOI: 10.1126/science.adq8590

CrSBr: vdW antiferromagnetic semiconductor

Triaxial anisotropy along a, b, c crystal axes.

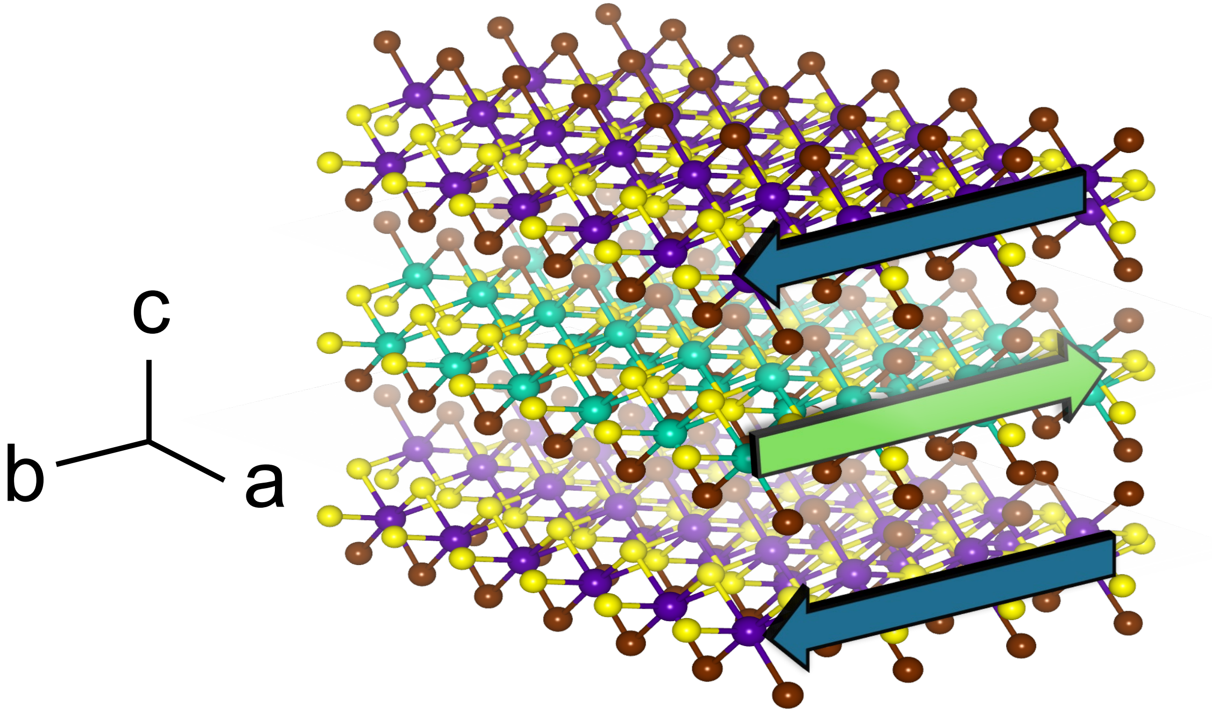

Microwave Transmission (Bulk Crystal)

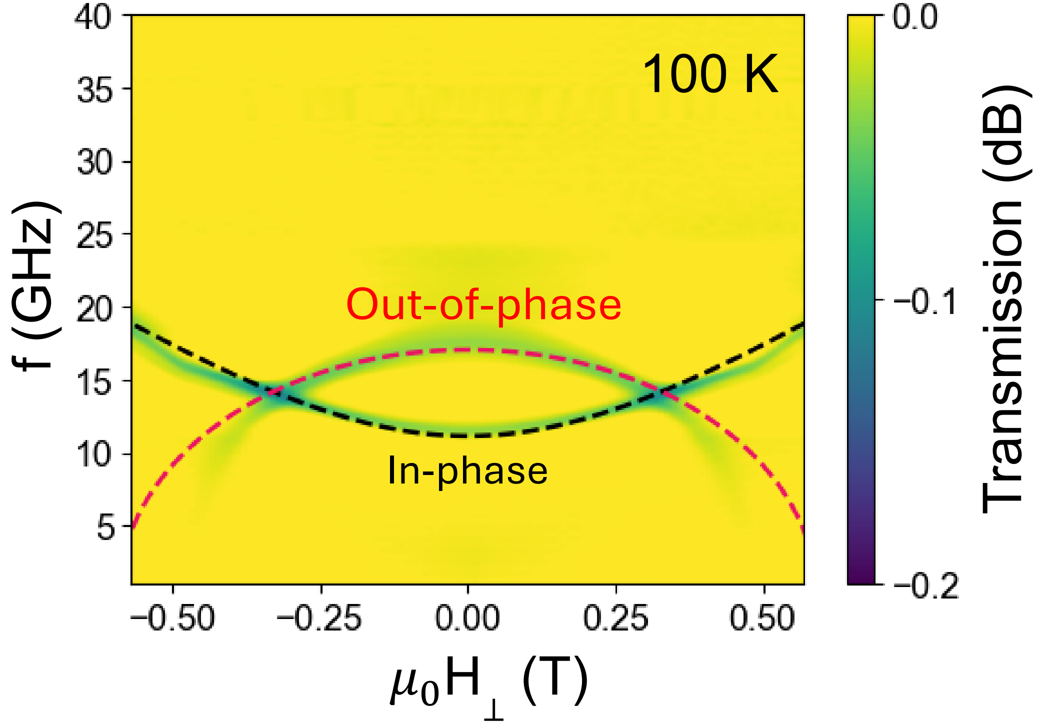

Telford, E.J. et al. 2020. *Advanced Materials*, *32*(37), p.2003240.

Lee, K. et al. *Nano Letters*, *21*(8), pp.3511-3517.

Our work: Cham, T. M. J., Ralph, D. C., & Luo, Y. K. et al. *Nano Letters* 22.16 (2022): 6716-6723.

Is it possible to detect these modes down to atomically thin layers?

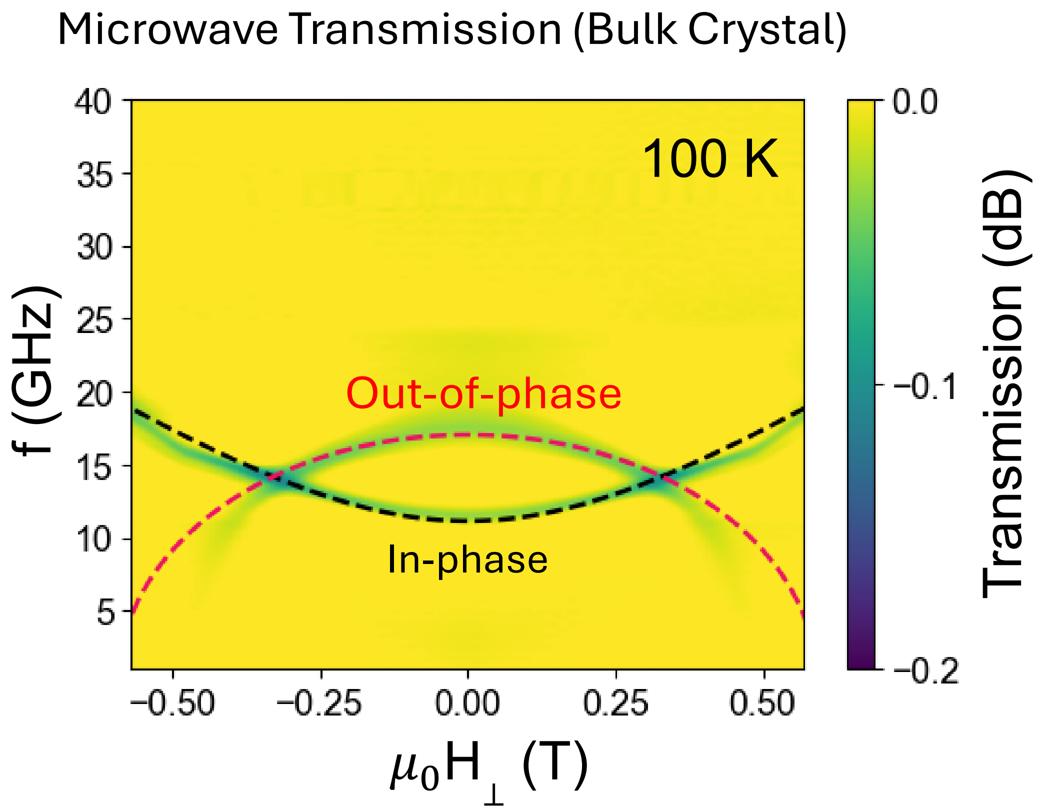

Spin Torque Ferromagnetic Resonance (ST-FMR)

Liu, L., Moriyama, T., Ralph, D. C., & Buhrman, R. A. (2011). Spin-torque ferromagnetic resonance induced by the spin Hall effect. *Physical review letters*, *106*(3), 036601.

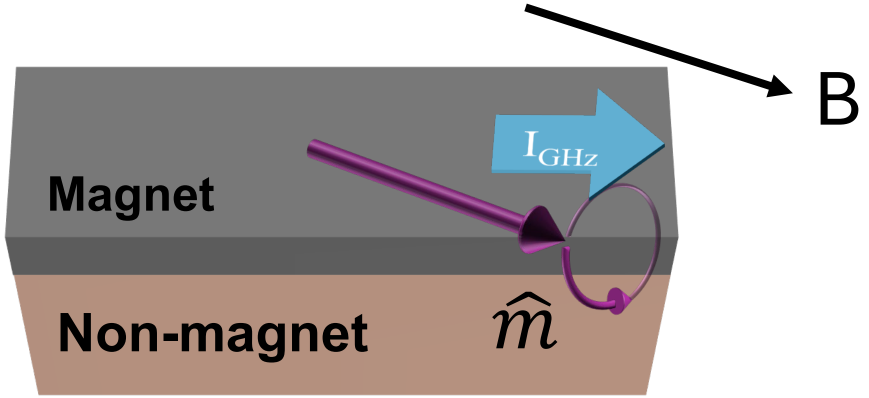

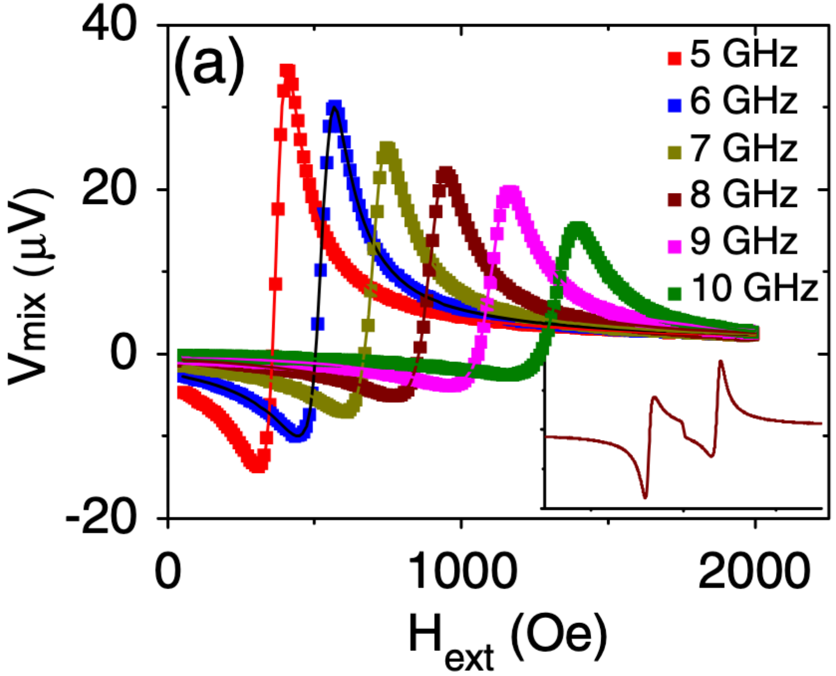

Kittel formula: $\omega_{resonance} = \gamma\sqrt{B\ (B + M_{eff})}$

Rectification Voltage Readout:

GHz Current

Anisotropic Magnetoresistance

$$V_{Rectified}(t) = I_0 \sin(\omega t)\,(R_0 + \Delta R \sin(\omega t)) = \frac{\Delta R I_0}{2} + O(\omega t)$$

Lorentzian components

$$V_{Rectified}^{DC} \propto S\frac{\Delta^2}{\Delta^2 + (B - B_0)^2} + A\frac{B(B - B_0)\Delta}{\Delta^2 + (B - B_0)^2}$$

Spin-filter tunneling magnetoresistance of CrSBr

Klein, D. R. et al. *Science* 360, 1218-1222 (2018)
Song, T. et al. *Science*, 360, 1214-1218 (2018)
Boix-Constant et al, *Advanced Materials*, *34*(41), 2204940 (2022)

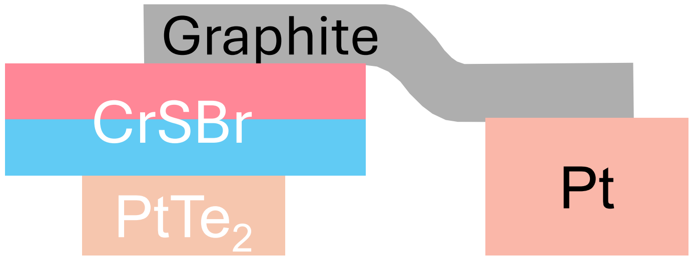

3-Terminal vdW Heterostructure Device:

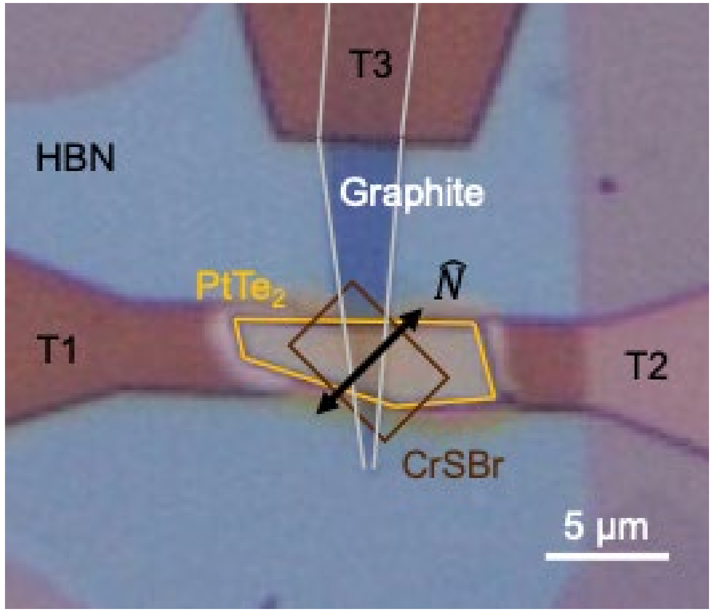

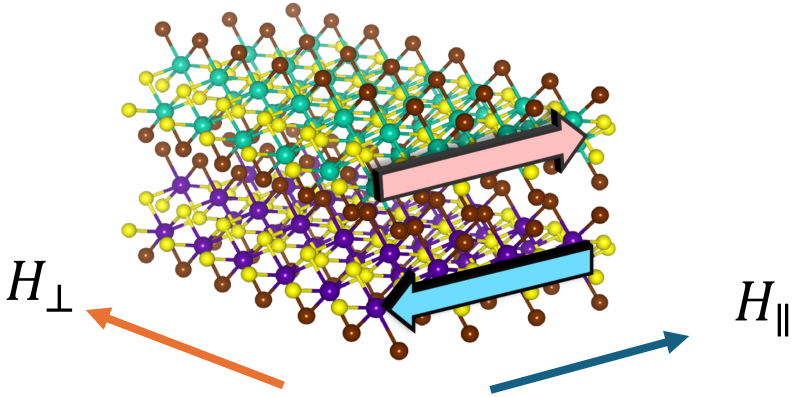

Spin-filter Tunneling Magnetoresistance

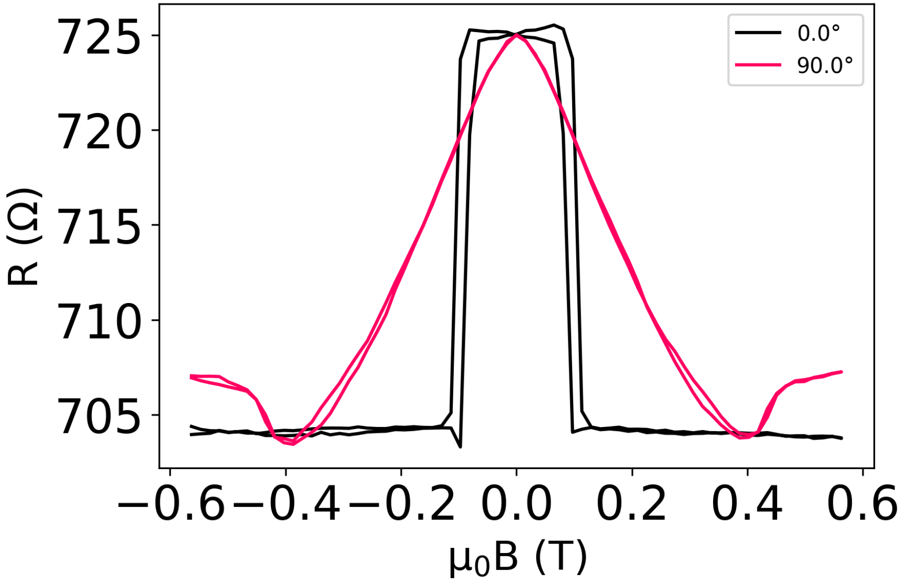

***arXiv:2407.09462*. Science (2025). DOI: 10.1126/science.adq8590**

Electrical Detection of Antiferromagnetic Resonance

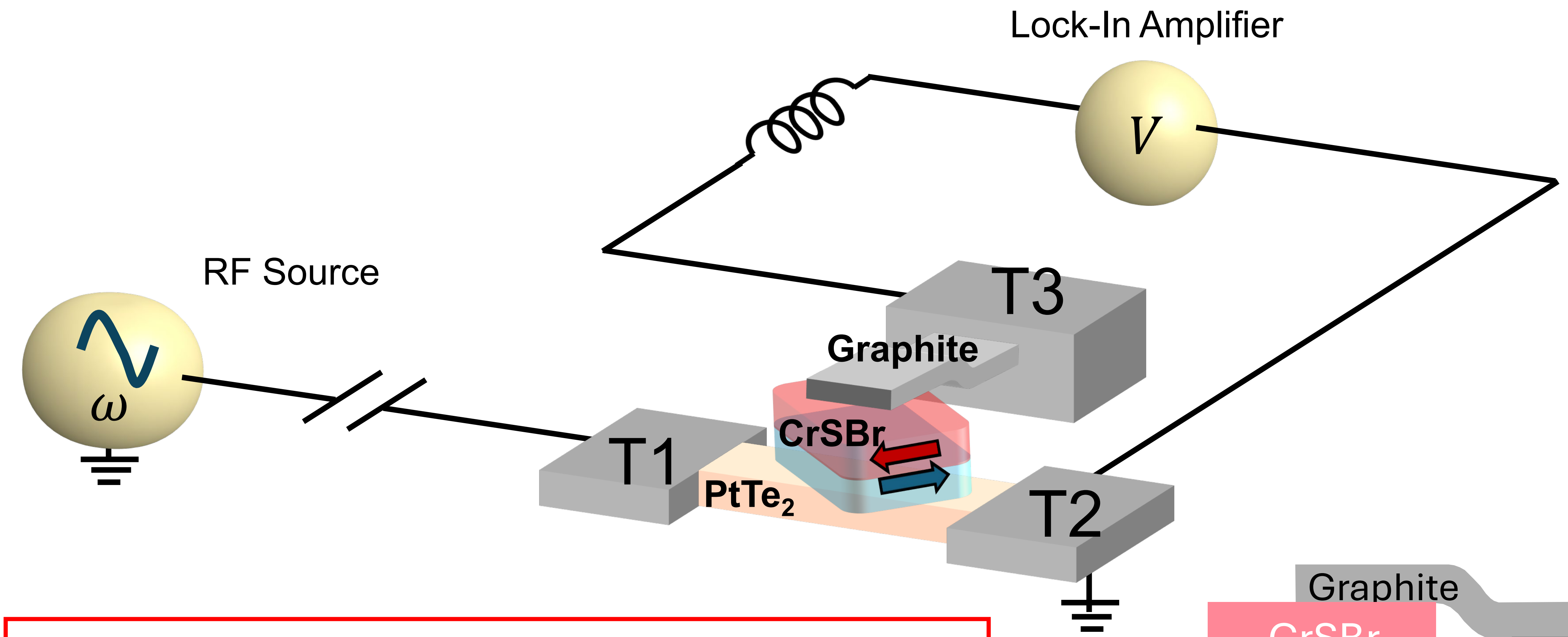

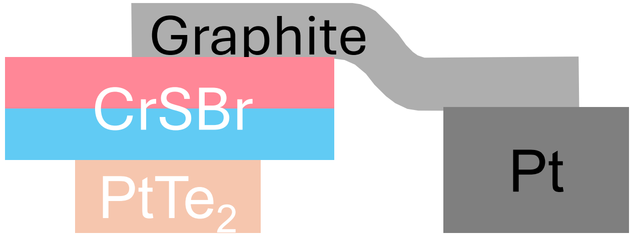

RF Current — Spin-filtering Magnetoresistance

$$V_{Rectified}(t) = \underbrace{I_0 \sin(\omega t)}_{\text{RF Current}} \underbrace{(R_0 + \Delta R \sin(\omega t))}_{\text{Spin-filtering Magnetoresistance}} = \frac{\Delta R I_0}{2} + O(\omega t)$$

Resonance Spectrum of Bilayer CrSBr

RF Current — MR Response

$$V_{mix}(t) = \mathrm{I}_0\sin(\omega t)(R_0 + \Delta R\sin(\omega t))$$

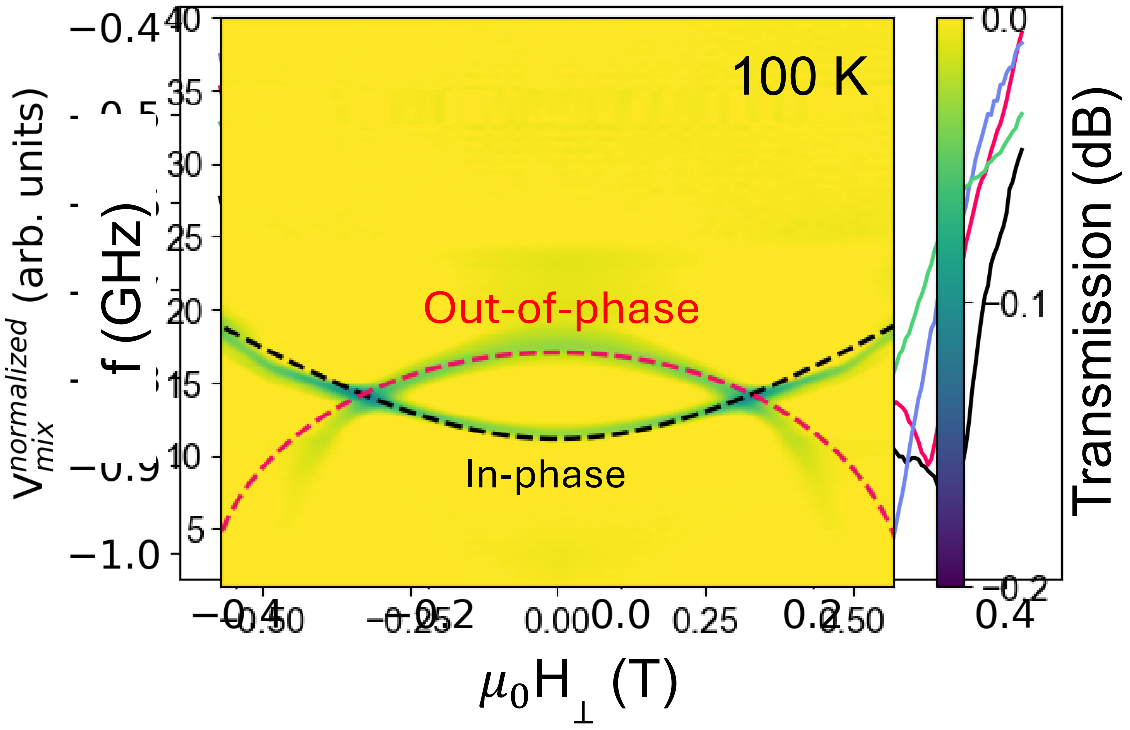

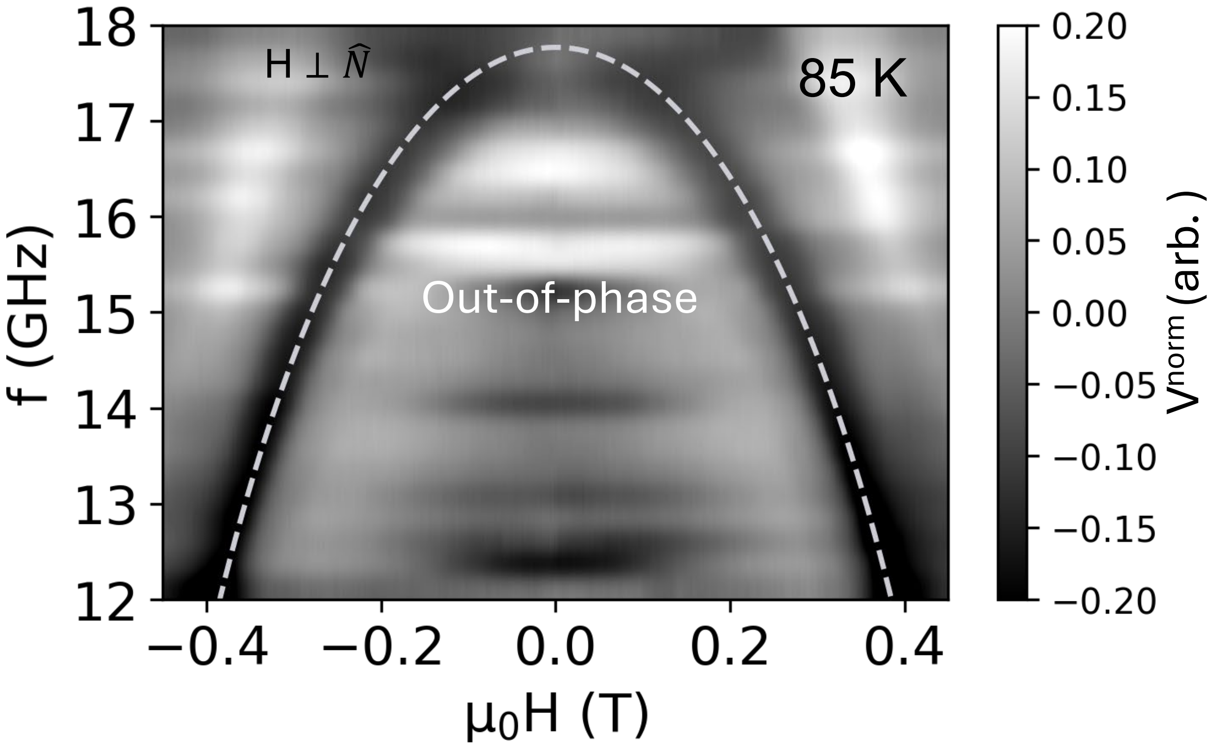

Spin filtering tunneling junction: electrical detection of out-of-phase AFMR modes in Bilayer CrSBr

Nano Letters **22.16 (2022): 6716-6723.**

***arXiv:2407.09462*. Science (2025). DOI: 10.1126/science.adq8590**

Spin-Orbit Torque Control of Antiferromagnetic Resonance

1 Electrical detection of AFMR using spin-filter tunneling resistance

2 Spin-Orbit torque Modulation of Antiferromagnetic Resonance

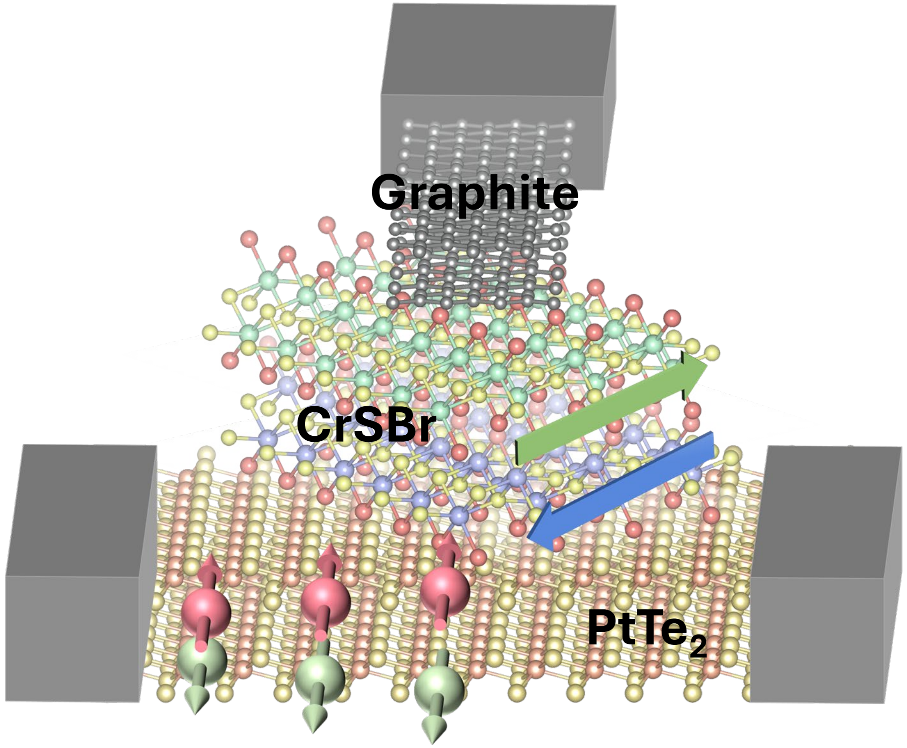

Cham, T. M. J., Huang, X., Chica, D. G., Watanabe, K., Taniguchi, T., Roy, X., Luo, Y. K., & Ralph, D. C. "Spin-filter tunneling detection of antiferromagnetic resonance with electrically-tunable damping" *arXiv:2407.09462*. Science (2025). DOI: 10.1126/science.adq8590.

Spin-torque modulation of magnetic damping

Liu, L., Moriyama, T., Ralph, D. C., & Buhrman, R. A. (2011). Spin-torque ferromagnetic resonance induced by the spin Hall effect. *Physical review letters*, *106*(3), 036601.

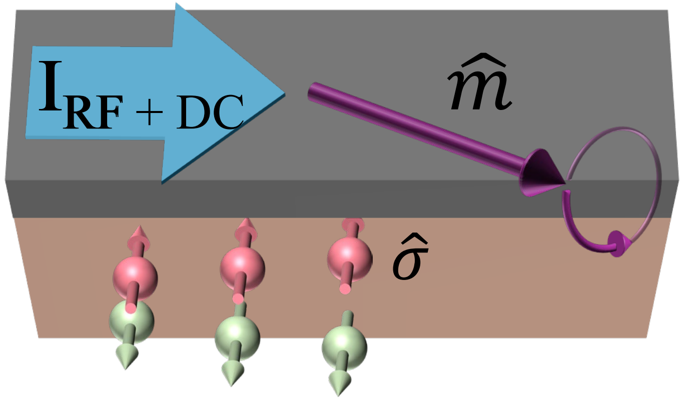

$$V_{rectified} \propto S\frac{\Delta^2}{\Delta^2 + (B - B_0)^2} + A\frac{\Delta^2}{\Delta^2 + (B - B_0)^2}$$

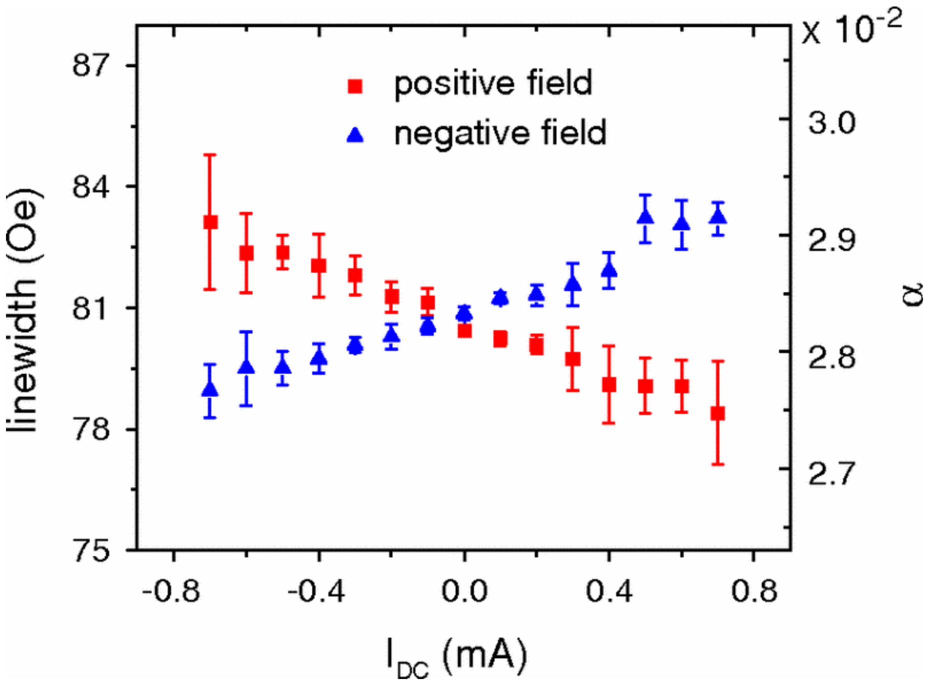

$$\Delta \propto (\alpha + A\xi_{SH} I_{DC} \hat{\sigma} \cdot \hat{m})$$

Δ: Lorentzian linewidth
α: Gilbert damping from SOC
ξ_{SH}: Spin torque efficiency
I_{DC}: DC bias current
$\hat{m}$: Magnetization
$\hat{\sigma}$: Spin polarization

Modulated linewidth scales linearly with DC current, proportional to ξ_{SH}
Changes sign with $m \cdot \sigma$

3-Terminal Geometry for AFMR Measurements in a vdW Heterostructure

Xue, L., Wang, C., Cui, Y. T., Liu, L., Swander, A., Sun, J. Z., ... & Ralph, D. (2012). Resonance measurement of nonlocal spin torque in a three-terminal magnetic device. *Physical Review Letters*, *108*(14), 147201.

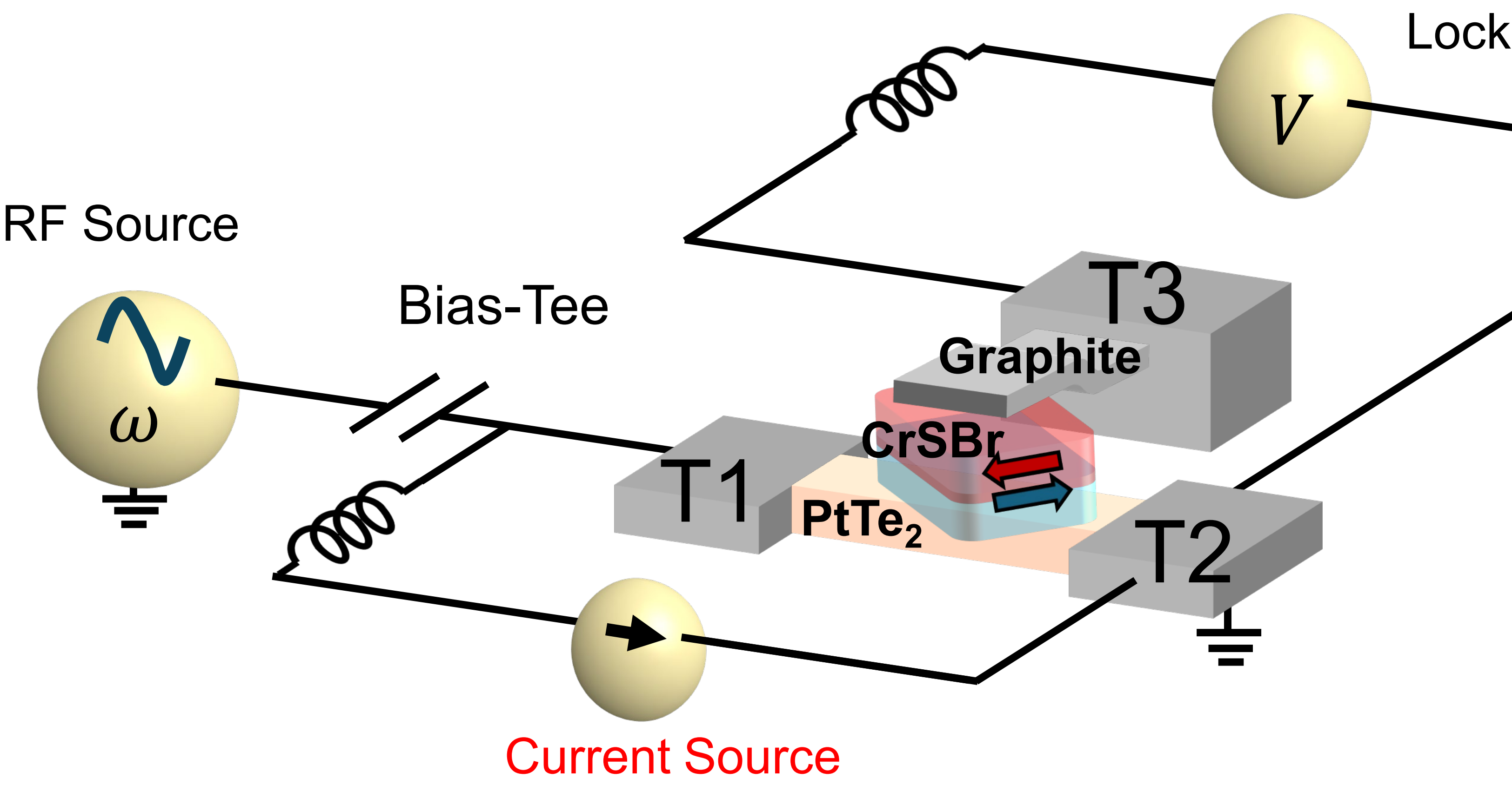

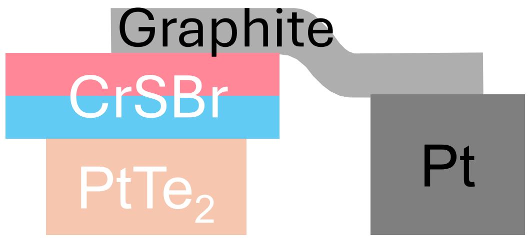

DC current generates spin current through $PtTe_2$ into CrSBr

AFMR linewidth modulation

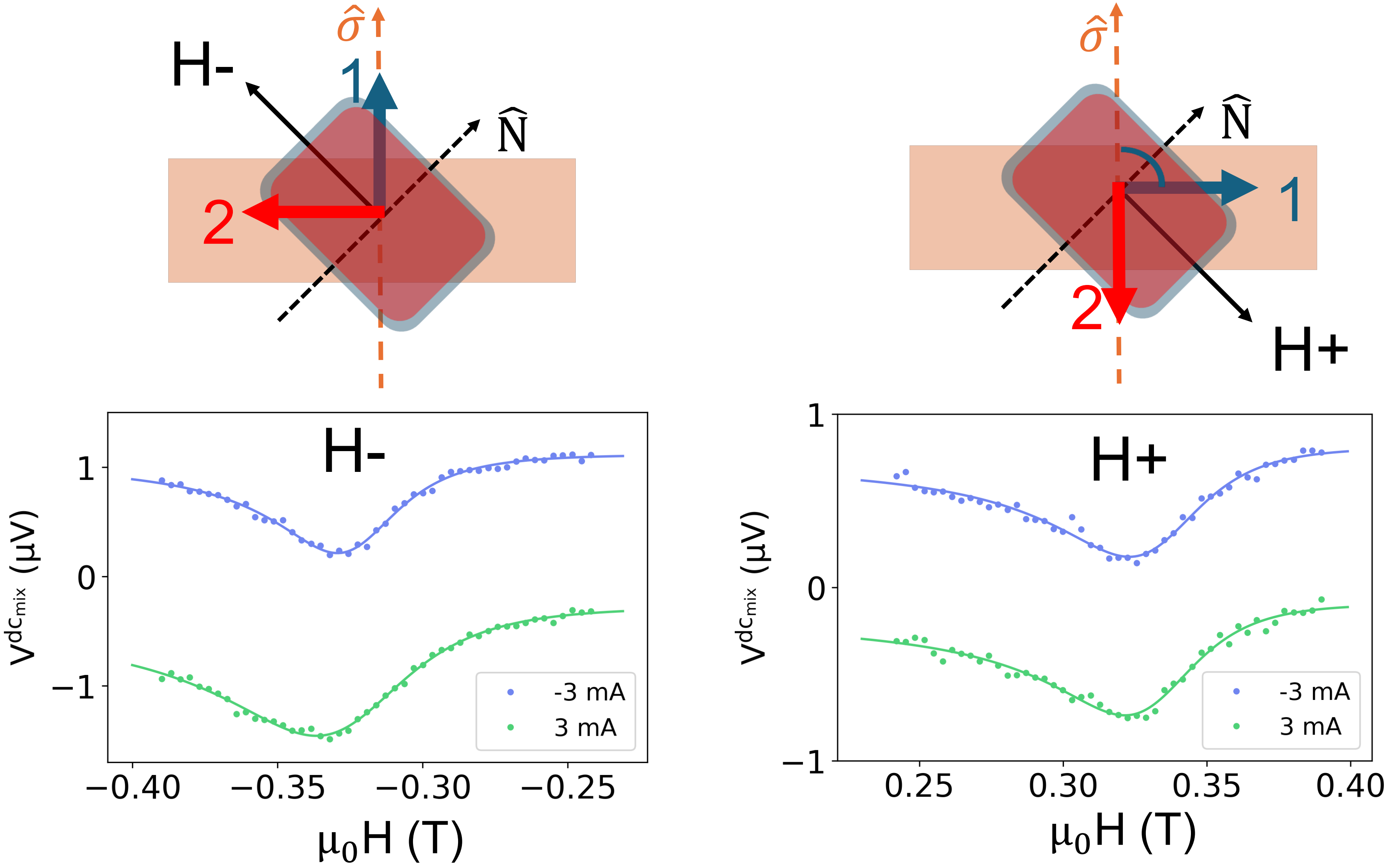

Linewidth is modulated only for the H- configuration.

***arXiv:2407.09462*. Science (2025),**
DOI: 10.1126/science.adq8590

AFMR linewidth modulation

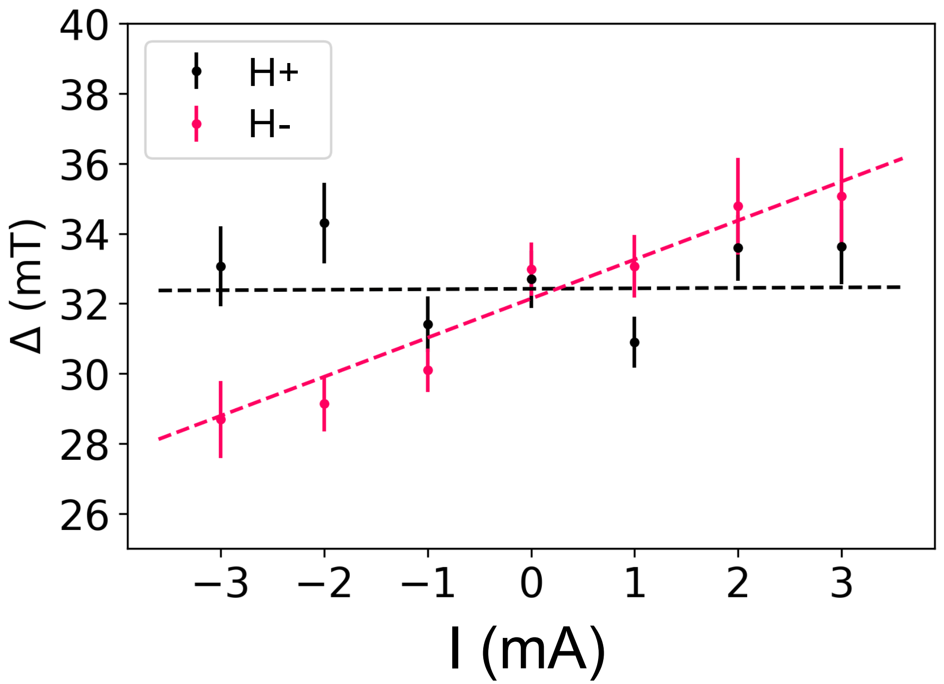

Current induced linewidth modulation slopes are different for H+ and H- fields
→ Suggests that **torques are only acting on the interfacial sublattice layer**

$$\frac{d\Delta}{dI} \propto \xi_{SH} \sigma \cdot \hat{m}_1 \quad \rightarrow \quad \xi_{SH} = 0.29(2)$$

Torque efficiency is comparable with SOT on ferromagnets

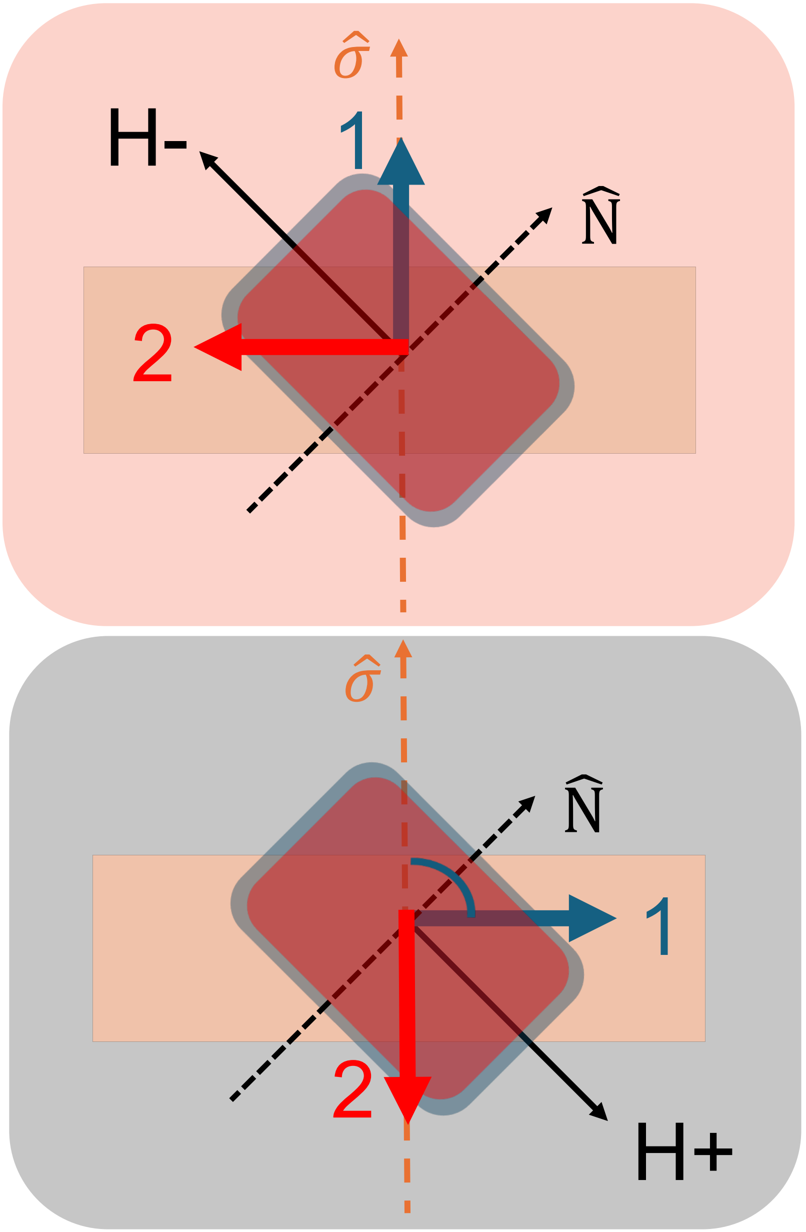

***arXiv:2407.09462*. Science (2025), DOI: 10.1126/science.adq8590.**

Summary and Outlook

- Electrical detection of AFMR in bilayer CrSBr.
- SOT acts primarily on interfacial sublattice layer of AFM.
- SOT efficiency on CrSBr is comparable with effect on ferromagnets.

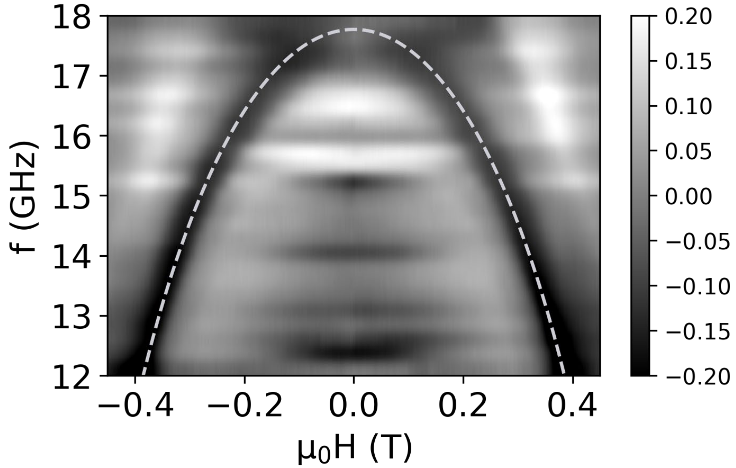

- Future opportunities for investigating AFM dynamics in 2D heterostructures
- Nanoscale GHz-THz AFM oscillators

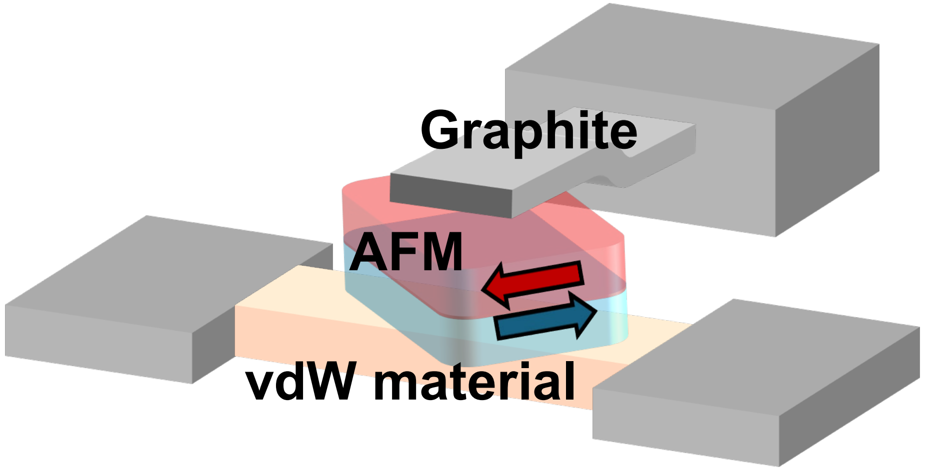

Cham, T. M. J., Huang, X., Chica, D. G., Watanabe, K., Taniguchi, T., Roy, X., Luo, Y. K., & Ralph, D. C. "Spin-filter tunneling detection of antiferromagnetic resonance with electrically-tunable damping" *arXiv:2407.09462*. Science (2025), DOI: 10.1126/science.adq8590

See our related works at: *Nano Letters, 22*(16), 6716-6723 (2022); *Advanced Materials*. 2305739 (2024)

Outline

Electrical detection of antiferromagnetic resonance with electrically-tunable damping

Nano Letters, *22*(16), 6716-6723 (2022);
Advanced Materials. 2305739 (2024)
arXiv: 2407.09462. Science (2025), in print

High-sensitivity optical SOT metrology: Sagnac Kerr interferometry

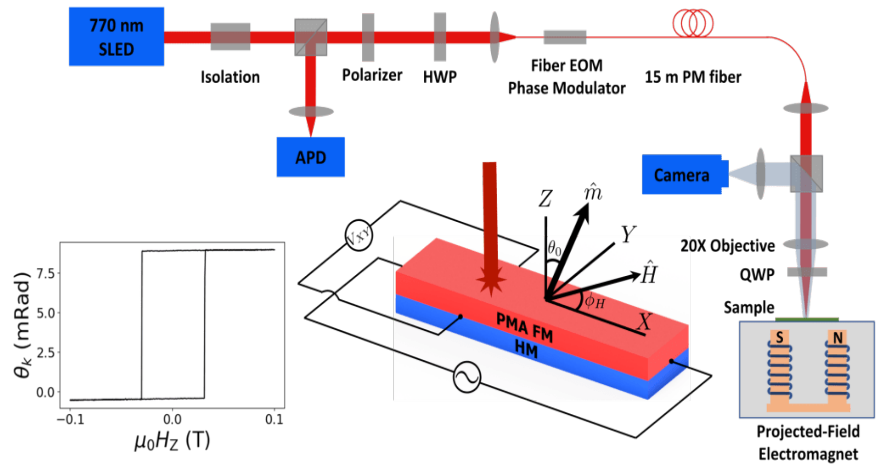

Science Advances **9(36), eadi9039 (2023);**
First version: arXiv: 2109.13759 (2021)

High-sensitivity magneto-optic DC readout: Sagnac optical interferometry

At least 50-100x better signal-to-noise than conventional DC MOKE magnetic imaging.

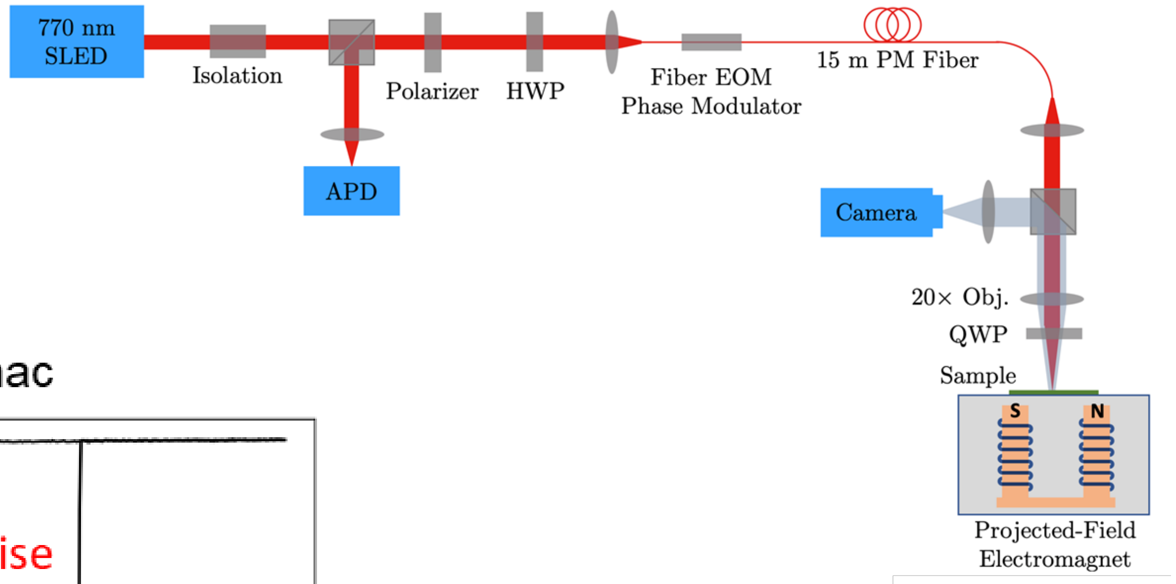

Conventional polar-MOKE signal

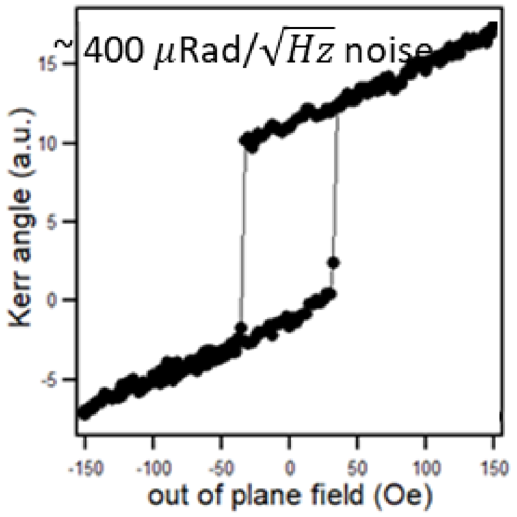

Sagnac

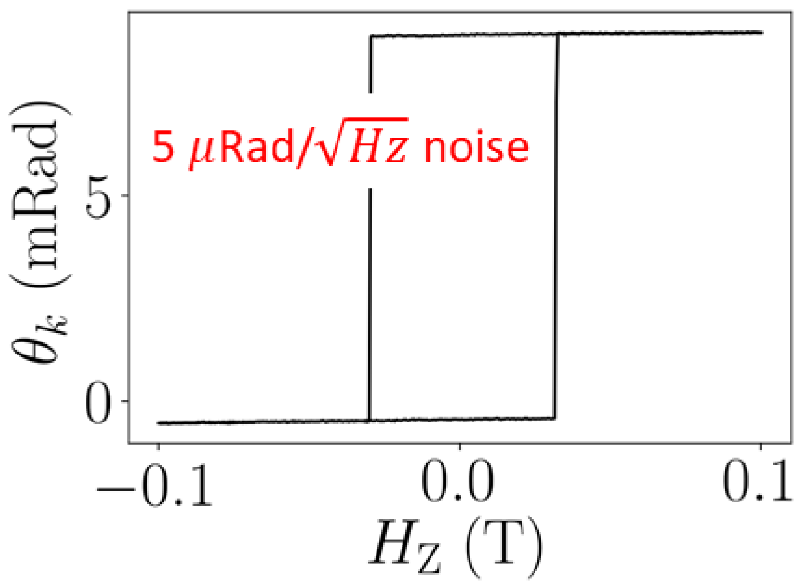

Science Advances **9(36), eadi9039 (2023);**
First version: arXiv: 2109.13759 (2021)

Substrate/Ta(1.5)/Pt(4)/Co(0.85-1.3)/MgO(1.9)/Ta(2)

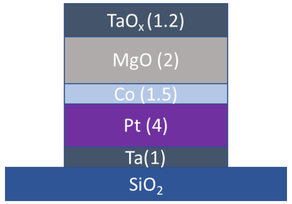

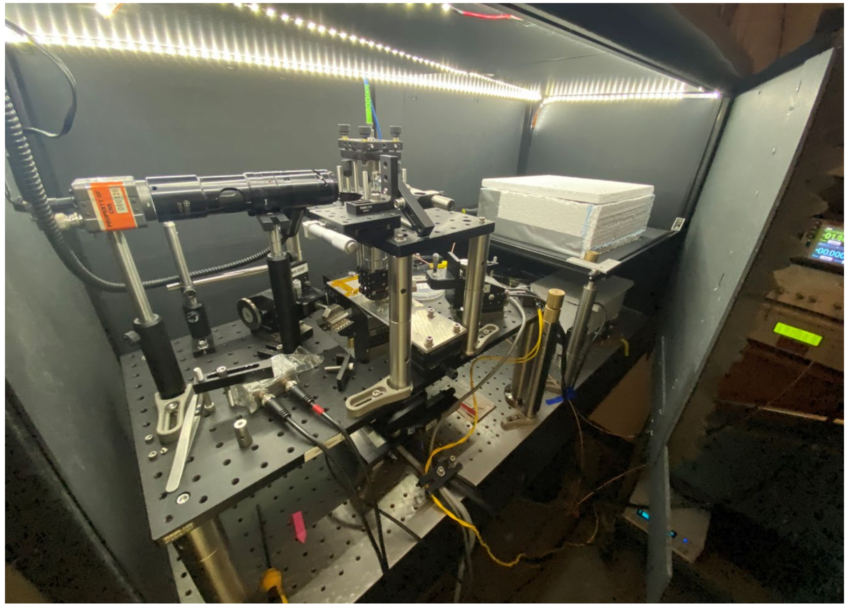

The setup:

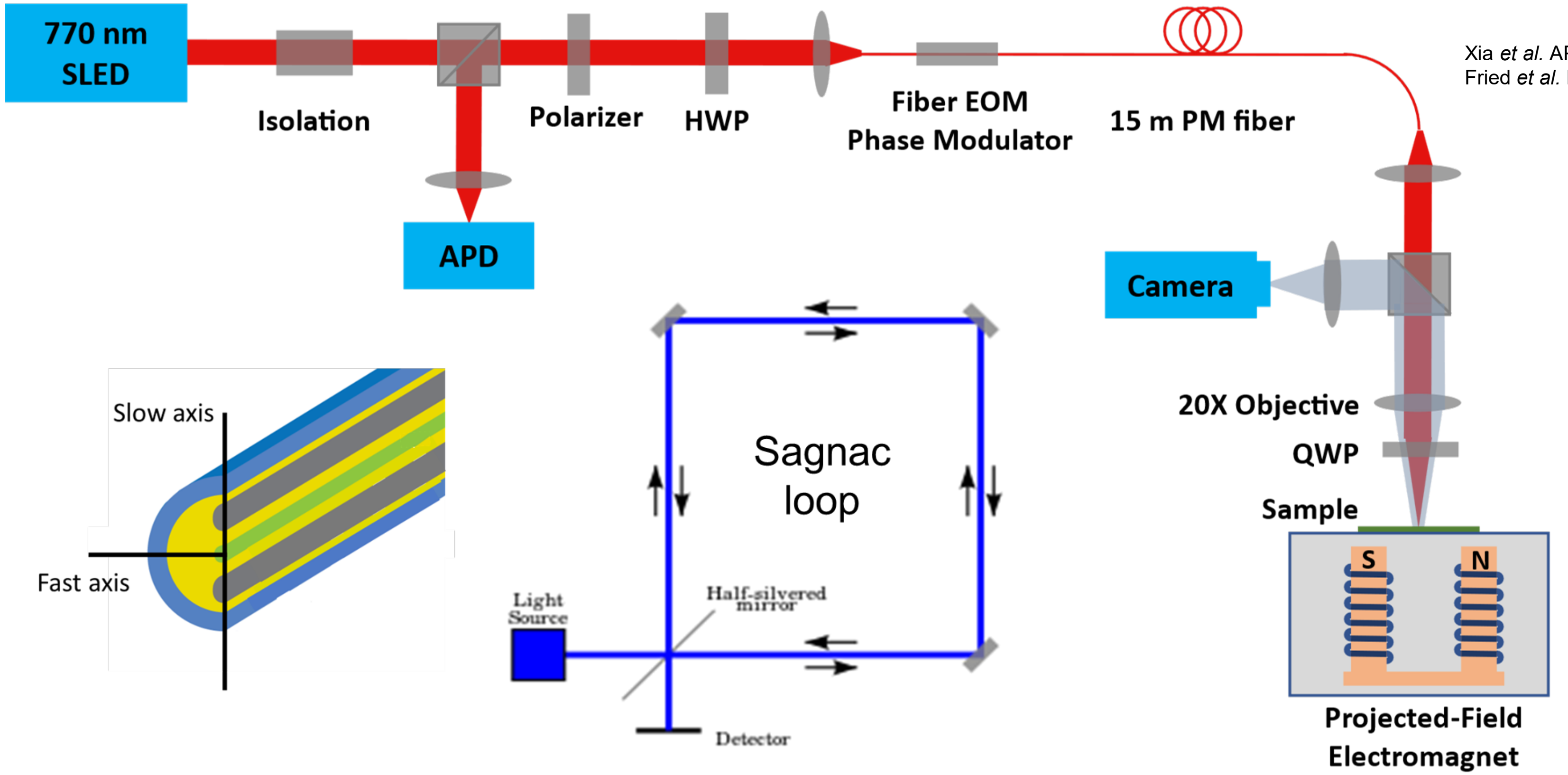

Xia *et al.* APL (2006)
Fried *et al.* Rev. Sci. Instrum. (2014)

- Two spatially overlapped, orthogonally polarized beams travel inside a single-mode polarization-maintaining (PM) fiber along its fast and slow axes.
- Two beams experience different phase modulation depth (ϕ_m = ϕ_{fast}- ϕ_{slow}) by an electro-optic phase modulator (EOM) at the modulation frequency w: $\phi_{fast}\sin(wt)$, $\phi_{slow}\sin(wt)$.
- Upon sample reflection, both beams pass the quarter-wave plate (QWP) twice, and travel back along opposite fiber axes to acquire same optical path with a phase difference: $(\phi_{fast} - \phi_{slow})\{\sin[w(t+\tau)] - \sin(wt)\}$, hence forming a Sagnac loop.

Kerr signal detection:

- We tune EOM frequency, w, such that $\tau = \pi/w$, and τ is the time of flight for the 30-meter fiber loop. Sample Kerr rotation can be quantified by 1st and 2nd harmonic interference intensity signals (I^w & I^{2w}):

Kerr rotation

$$I^{\omega} = -\frac{\sin 2\theta_k J_1(2\phi_m)}{4r_- r_+}$$

Kerr ellipticity

Kerr rotation

$$I^{2\omega} = -\frac{\cos 2\theta_k J_2(2\phi_m)}{4r_- r_+}$$

Kerr ellipticity

$$\theta_k = \frac{1}{2}\tan^{-1}\left[\frac{J_2(2\phi_m)I^{\omega}}{J_1(2\phi_m)I^{2\omega}}\right]$$

J_1,J_2: Bessel-J functions

Ultrasensitive out-of-plane magnetization: absence of in-plane magnetization detection

Transport Hall voltage ← simultaneously → Sagnac Kerr signal

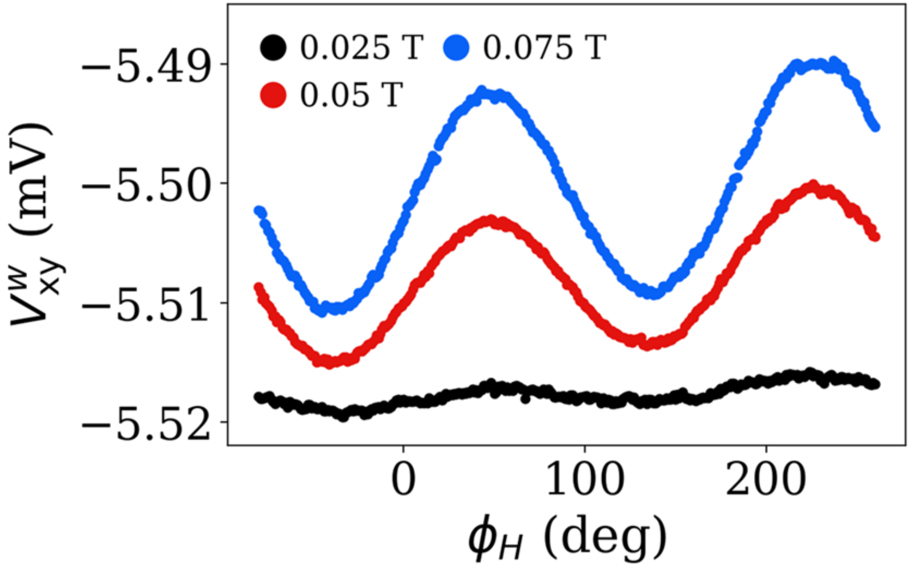

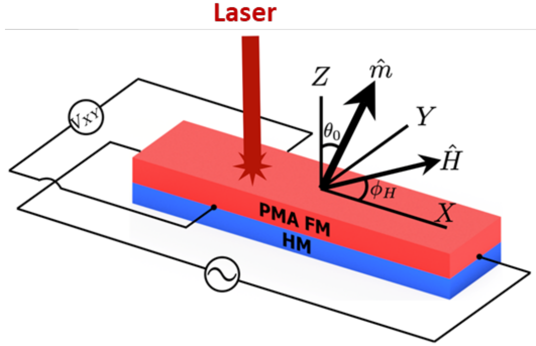

Angle dependence due to a small field/sample tilt.

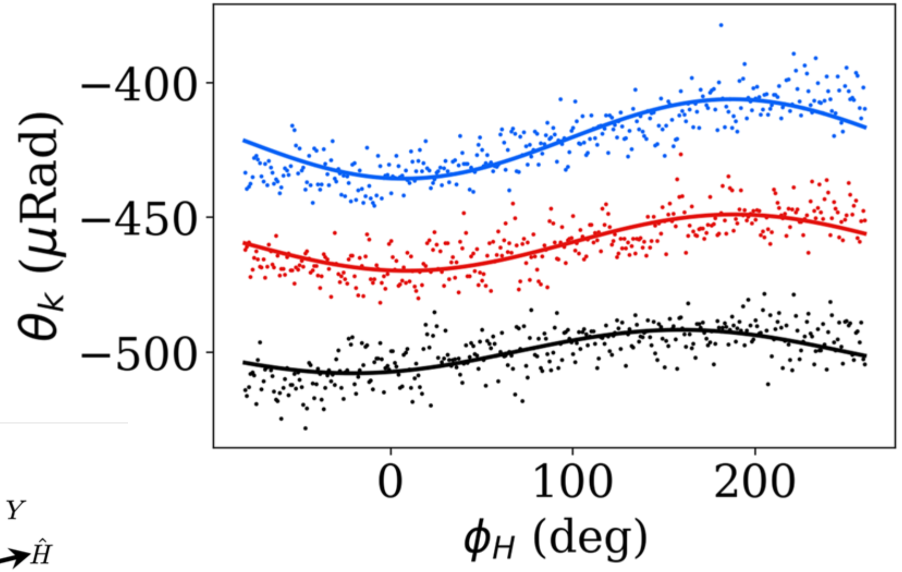

$$V^{\omega}_{XY} = \Delta I R_{\mathrm{AHE}} m_Z + \Delta I R_{\mathrm{PHE}} m_X m_Y$$

Harmonic Hall commonly give inconsistent results due to artifacts associated with planar Hall effect R_{PHE}

$$\theta_k = \kappa m_z + \beta_Q m_x m_y$$

Estimated a factor of 10^{-4} smaller than κm_Z

See details in the SI: Science Advances 9(36), eadi9039 (2023)

See details in our first version: arXiv: 2109.13759 (2021)

Using Sagnac interferometry to measure spin-orbit torques

Based on the steady-state Landau-Lifshitz-Gilbert-Slonczewski (LLGS) macrospin equation, we determine the current-induced damping-like and field-like effective torques (per unit magnetization) τ_{DL}^{0} and τ_{FL}^{0} by balancing the following equation:

$$\gamma\mu_0\Delta\hat{m} \times \vec{H}_{\text{eff}} = \tau_{\text{DL}}^{0}\hat{m} \times (\hat{\sigma} \times \hat{m}) + \tau_{\text{FL}}^{0}\hat{\sigma} \times \hat{m}$$

Samples with perpendicular magnetic anisotropy

$$\theta_k = \pm\kappa\left(1 - \frac{H^2}{2M_{\text{eff}}^2}\right)$$

- Sagnac Kerr rotation θ_k sensitively measures changes in the OOP magnetization m_z that are **second order in small-angle tilting from the OOP direction**.

Samples with in-plane magnetic anisotropy

$$\Delta\theta_k = \frac{\kappa\Delta H_{\text{DL}}\cos\phi_H}{H - M_{\text{eff}}}$$

- The current-induced changes in m_z are **first order in the OOP tilting angle**.

Tilting from applied external magnetic fields

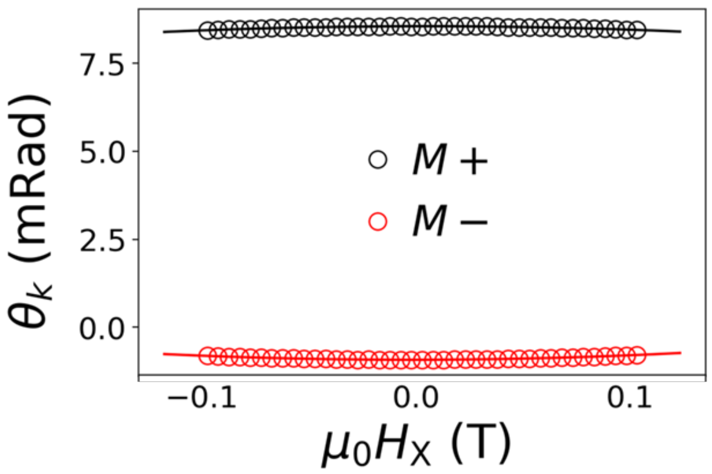

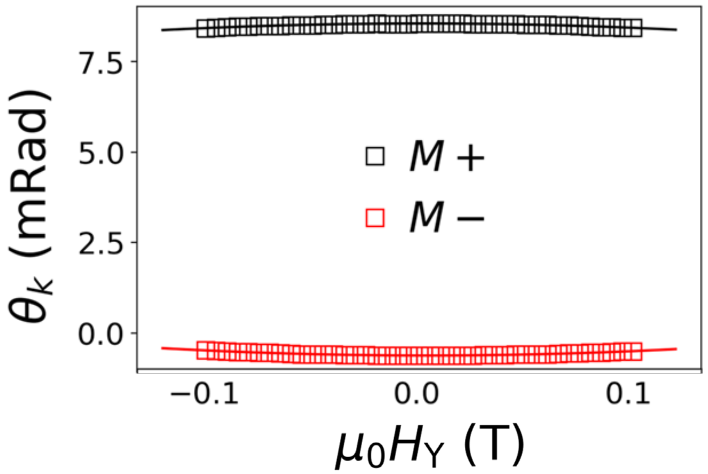

Samples with perpendicular magnetic anisotropy

$$\theta_k \approx \pm\kappa\left(1 - \frac{H_{X(Y)}^2}{2\mu_0^2 M_{\mathrm{eff}}^2}\right)$$

κ: a coupling constant between m_Z and θ_k, analogous to R_{AHE}.

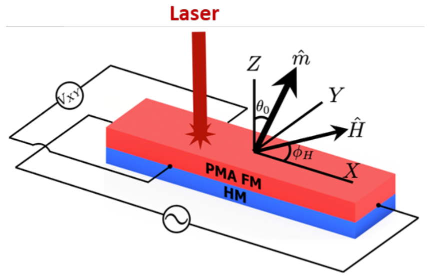

Tilting from current induced M_z motion

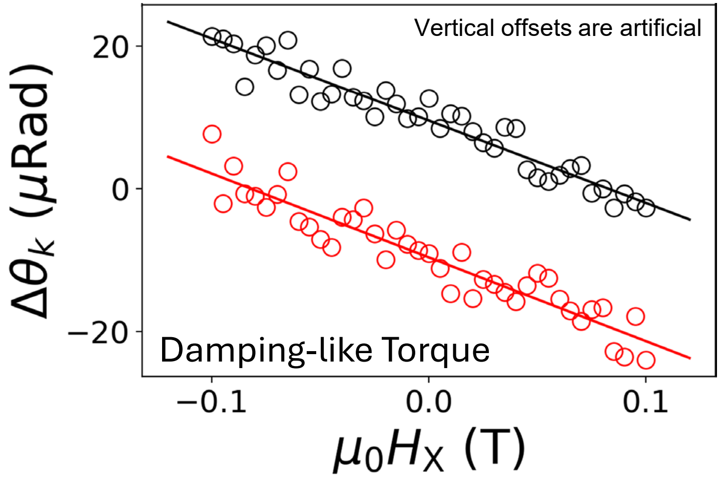

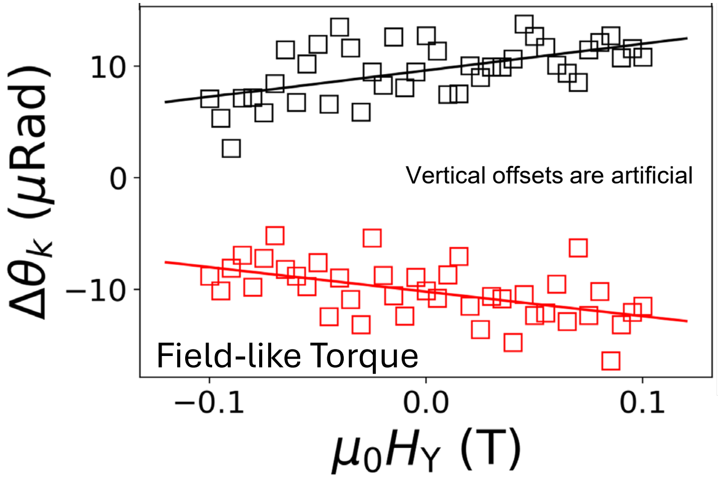

Slope measures the spin-torque effective magnetic field $\Delta H_{X(Y)}$

Current-induced Kerr signal:

$$\Delta\theta_k \approx \pm\kappa\Delta H_{X(Y)}\frac{H_{X(Y)}}{\mu_0^2 M_{\mathrm{eff}}^2}$$

$$\mu_0\Delta H_X = \mp\tau_{\mathrm{DL}}^0/\gamma$$

$$\mu_0\Delta H_Y = \mu_0 H_{\mathrm{Oe}} + \tau_{\mathrm{FL}}^0/\gamma$$

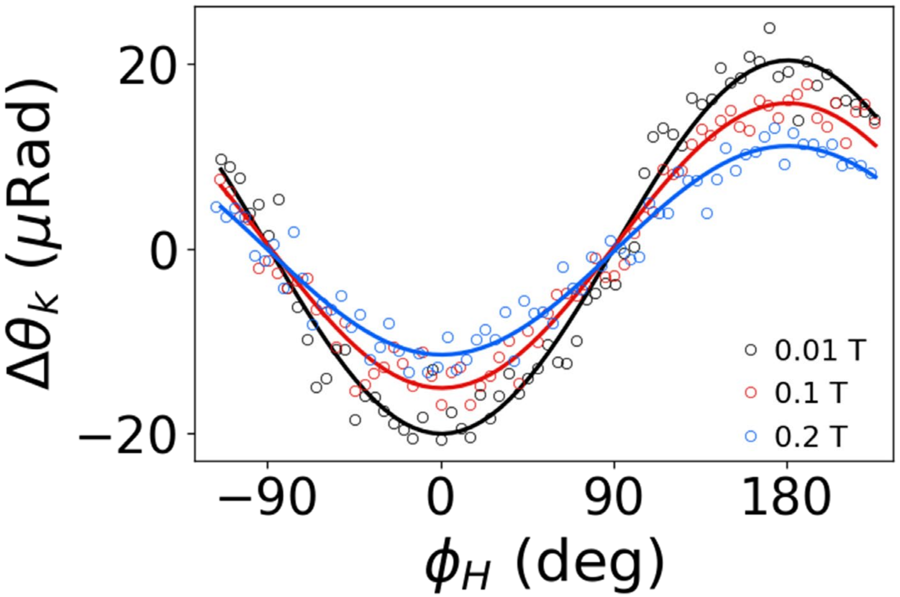

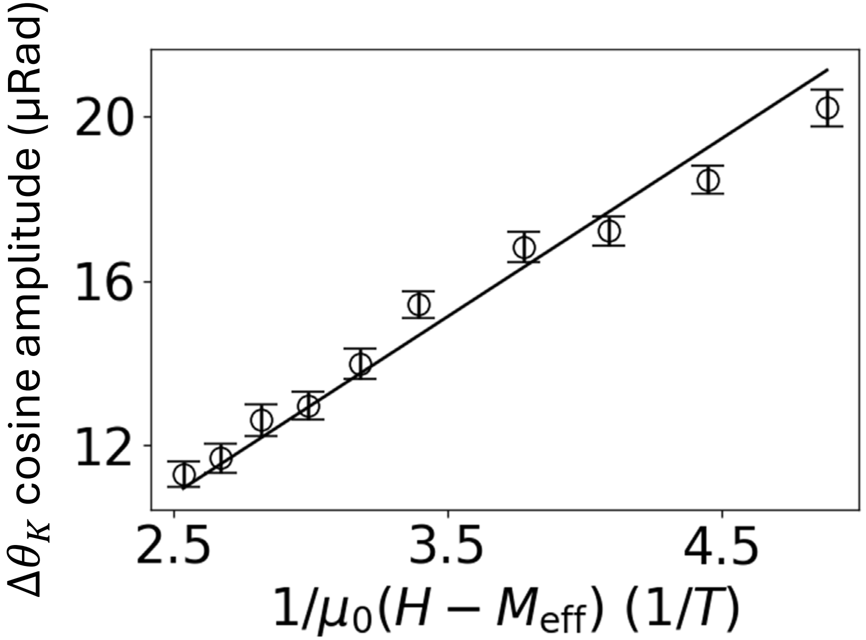

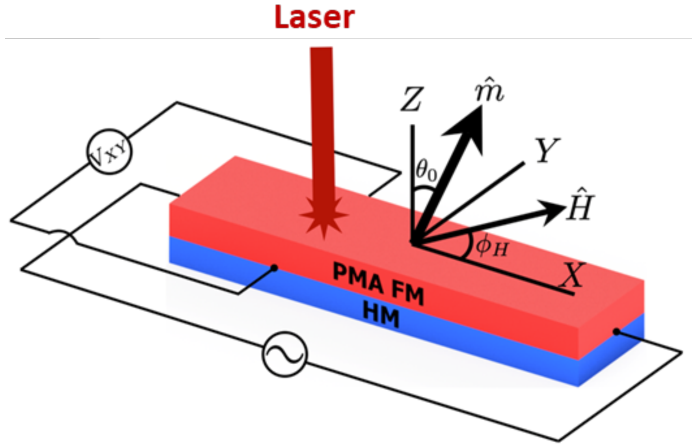

Samples with in-plane magnetic anisotropy

$$\Delta\theta_k = \frac{\kappa \Delta H_{\mathrm{DL}} \cos\phi_H}{H - M_{\mathrm{eff}}}$$

- The current-induced changes in m_Z are **first order in the OOP tilting angle**.
- Damping-like torque (τ_{DL}^0) corresponds to an OOP effective field, while the field-like torque (τ_{FL}^0) gives an in-plane effective field.

Results for the damping-like (ξ_{DL}) and field-like (ξ_{FL}) spin-orbit-torque efficiencies for the sample series substrate/Ta(1.5)/Pt(4)/Co(0.85−2.1)/MgO(1.9)/Ta(2)

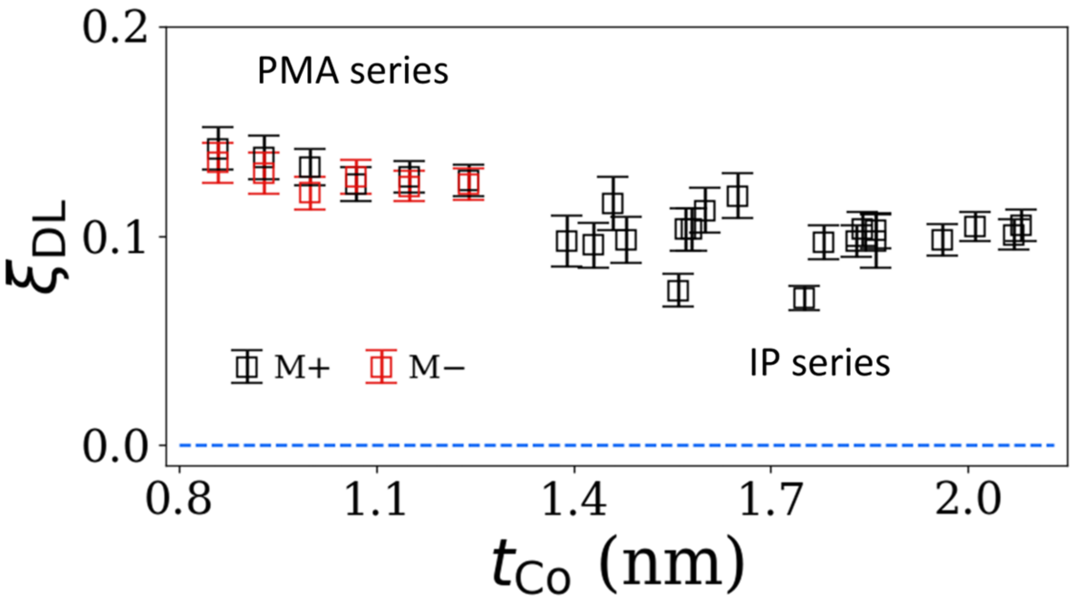

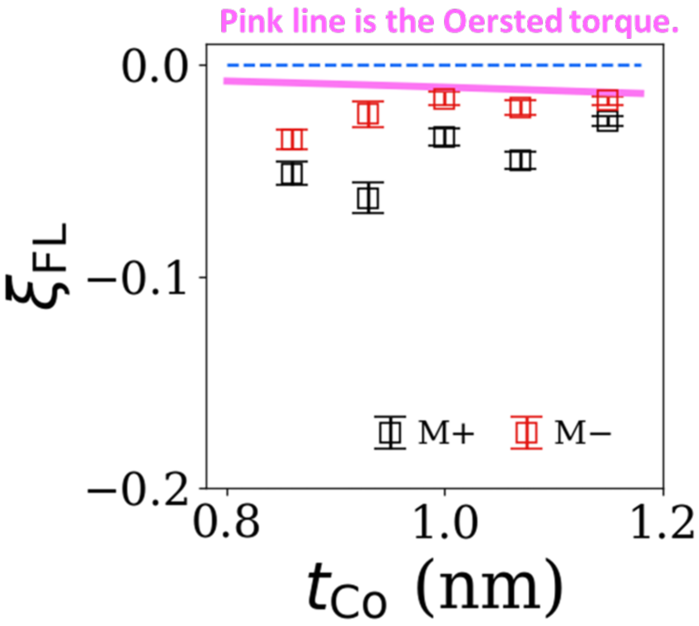

- Co thickness variation gives competition between in-plane shape anisotropy and interfacial perpendicular magnetic anisotropy (PMA), resulting in different values of effective magnetization M_{eff}.
- Sagnac results for damping-like torque efficiency ξ_{DL} on PMA and in-plane samples are consistent, which is often not the case for electrically-based measurements.

Karimeddiny, Cham, Smedley, Ralph, Luo, *Science Advances* 9(36), eadi9039 (2023);

See detailed discussions on harmonic Hall discrepancy in our first version: arXiv: 2109.13759 (2021)

Sagnac Kerr sensitivity for metallic v.s. insulating 3D magnets

Samples	Anisotropy	θ_k (mRad) as-grown	θ_k (mRad) after Pt sputtering	$\mu_0 M_{eff}$ (T) as-grown	$\mu_0 M_{eff}$ (T) after Pt sputtering
Ferromagnet metal: Pt (4 nm)/Co (1.4 nm)	Weakly PMA	N/A	8 (4nm Pt)	N/A	0.12 (4nm Pt)
Ferrimagnet insulator: Bi:YIG (9 nm) on GSGG substrate	PMA	0.54	0.25 (4nm Pt)	0.32	0.16 (4 nm Pt)
Ferromagnet insulator: LAFO (8.5 nm) on $MgGa_2O_4$ substrate	PMA	0.057	0.025 (2 nm Pt)	0.25	0.21 (2 nm Pt)

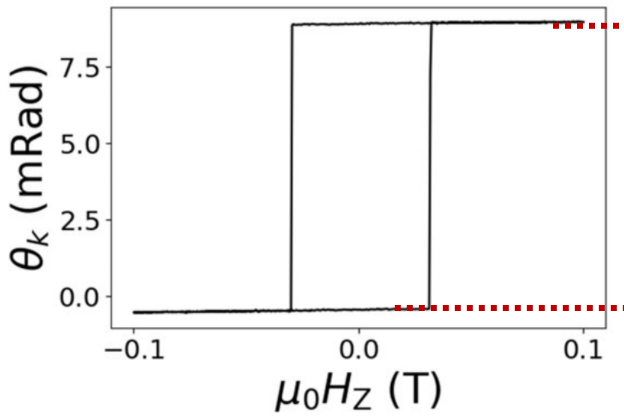

Sagnac sensitivity θ_k

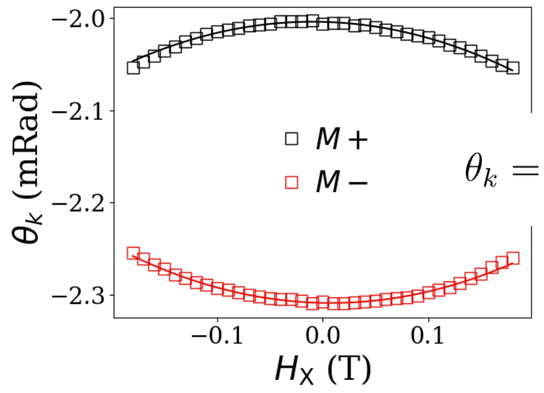

$$\theta_k = \pm\kappa\left(1 - \frac{H^2}{2M_{\rm eff}^2}\right)$$

Pt (4nm)/Bi:YIG (9 nm)

Cryo-Sagnac: towards high-efficiency SOT switching with 2D magnets

2D magnets: potential for ultralow current switching due to reduced net magnetization.

Cryo-Sagnac: outstanding probe especially for **insulating 2D magnets** due to challenging electrical readout.

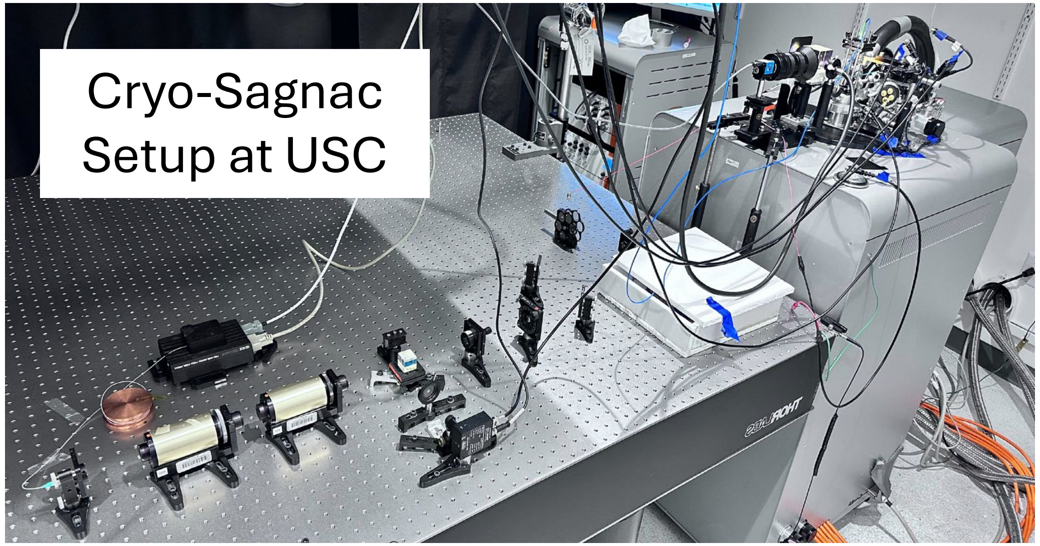

USC

- Variable sample temp: 1.7 – 320 K
- 9-1-1 T vector superconducting magnets

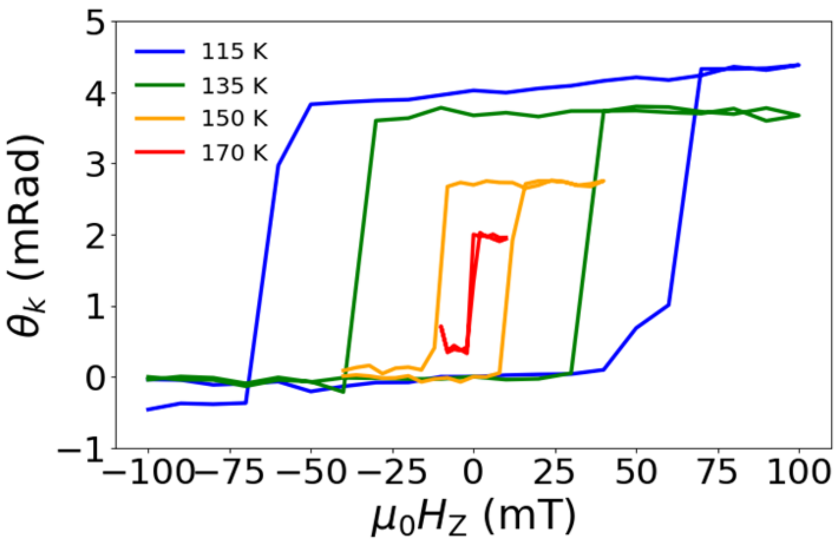

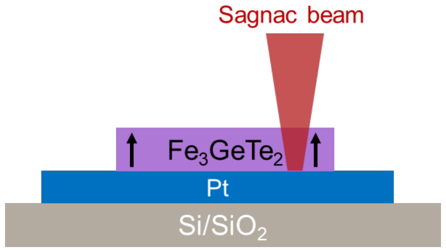

Fe_3GeTe_2 single crystal grown by Andrew May (Oakridge)

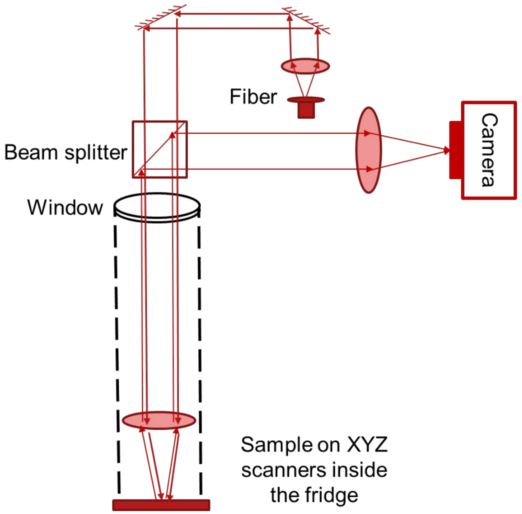

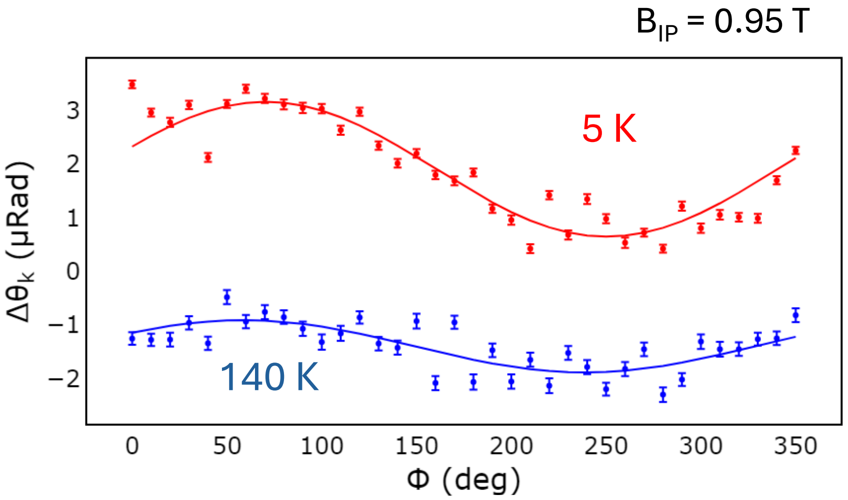

Spin torque on sample with in-plane anisotropy

$$\Delta\theta_k = \frac{\kappa \Delta H_{\mathrm{DL}} \cos\phi_H}{H - M_{\mathrm{eff}}}$$

Outstanding opportunities in multifunctional vdW heterostructures for spin-based quantum information processing

Next-gen spin-orbit torque MRAM devices based on altermagnetic and topological materials

Ultrafast spin, valley and magnon dynamics revealed by time-resolved Sagnac Kerr interferometry, tr-XMCD, and tr-ARPES

Air-free integration of vdW and non-vdW materials through collaborative thin film and bulk crystal growths

Superconducting spin torque for cryogenic memory

Ultrafast Quantum Opto-Spintronics Lab:
https://sites.usc.edu/kellyluolab/